Aus der Klinik und Poliklinik für Zahnerhaltung und Parodontologie der Ludwig-Maximilians-Universität München
Direktor: Professor Dr. Reinhard Hickel

und dem Walther-Straub-Institut für Pharmakologie und Toxikologie der Universität München
Vorstand: Professor Dr. Thomas Gudermann

Ti release from dental implants in human jawbone and the toxicity and cellular uptake of Ti particles in human cells

Dissertation
zum Erwerb des Doktorgrades der Naturwissenschaften
an der Medizinischen Fakultät der
Ludwig-Maximilians-Universität zu München

vorgelegt von
Xiuli He
aus People's Republic of China, Shandong
2016

Mit Genehmigung der Medizinischen Fakultät
der Universität München

Betreuer(in):	Prof. Dr. Dr. Franz-Xaver Reichl
Zweitgutachter:	Prof. Dr. Dennis Nowak
Dekan:	Prof. Dr. med. dent. Reinhard Hickel
Tag der mündlichen Prüfung:	21.03.2017

Einleitende Zusammenfassung

der schriftlichen, kumulativen Promotion

gemäß § 7 Abs. 4 der Promotionsordnung für die Promotion zum Dr. rer. nat.

an der Medizinischen Fakultät

Contents:

Abbreviations:

Ti	Titanium
Ni	Nickel
Cr	Chromium
Fe	Iron
Mo	Molybdenum
NiTi	Nickel Titanium
Ti-NPs	Titanium nanoparticles
Ti-MPs	Titanium microparticles
NiTi-MPs	Nickel Titanium microparticles
NPs	nanoparticles
hTERT	human telomerase reverse transcriptase
PDL	periodontal ligament
ICP-OES	inductively coupled plasma optical emission spectrometry
LA-ICP-MS	laser ablation-inductively coupled plasma-mass spectrometry
SEM	scanning electron microscope
EDX	energy dispersive X-ray
EC_{50}	half-maximum effect concentration
PBS	phosphate buffered saline
LSCM	laser scanning confocal microscopy
TEM	transmission electron microscopy
OTM	olive tail moment
SiTi	Silica-Titania Hollow

1 Introduction

1.1 Analysis of Ti and other metals in human jawbones with dental implants

Ti and its alloys have been widely used for dental and medical applications in the last 50 years [1, 2]. Clinically, pure Ti (Ti >99%) and the alloy Ti-6Al-4V are mainly used for endosseous implants [2]. Ti alloys with other metals (e.g. Ni, Cr, Fe and Mo) are applied for implant devices such as bone plates or screws [2, 3]. Ti becomes the mainly used component in those implants/implant devices, since the stable TiO_2 layer [4, 5] formed on the surface can provide Ti based implants/implant devices with high biocompatibility and resistance to corrosion [6-9].

Although Ti based implants are considered to be biologically inert, it has been found that implants in the body can undergo corrosion and release particulate debris over time [10, 11]. It has also been reported that the metallic debris from Ti based implants might exist in several forms including particles (micrometre to nanometre size), colloidal and ionic forms (e.g. specific/unspecific protein binding) [12, 13], organic storage forms (e.g. hemosiderin, which is an iron-storage complex), inorganic metal oxides and salts [12]. According to a previous study [14], the degradation of implants in the human body is primarily induced by wear and corrosion: wear is the mechanical/physical form of implant degradation which produces particles; while corrosion refers to the chemical/electrochemical form of degradation that mainly produces soluble metal ions [14]. Ti particles released from implants have been found in the regenerated bone and peri-implant tissues in animals [7, 15]. It has been shown that also Ti ions can be released from embedded implants in animals[16] [17]. Ti particles/ions are able to enter the circulation of blood and lymph [12, 18, 19]. Ti particles detached from hip, knee and mandible implants have been detected in organs such as liver, spleen, lung and lymph nodes [5, 19]. Increased levels of elementary Ti have also been detected in the blood of patients with poorly functioning implants [12].

Increased concentrations of metals (e.g. Ti, Cr, Co and Al) derived from implants in body fluids might induce acute or chronic toxicological effects [12]. The long-term effects of Ti derived from implants are still not fully understood, but associated hypersensitivity and allergic reactions in patients have been reported [20, 21]. In a clinical study, 0.6% of 1500 patients were found to exhibit Ti allergic reactions [20]. Additionally, it has been found that detached metal debris from implants might cause marrow fibrosis, necrosis and granulomatosis [22-24].

Therefore, the release of Ti and other metallic elements in human body from dental implants should be concerned and measured. In our study, Ti content released from implants inserted into human jawbones was measured, Ti particles released to bone/bone marrow tissues were identified, and the spatial distribution of Ti in human jawbones near implants was also

investigated. This work was illustrated in the following publication: He X, Reichl FX, Wang Y, Michalke B, Milz S, Yang Y, Stolper P, Lindemaier G, Graw M, Hickel R, Högg C. *Analysis of titanium and other metals in human jawbones with dental implants–A case series study.* Dent Mater. 2016; 32:1042-51.

1.2 Intracellular uptake and toxicity of three different Ti particles

Ti is preferentially used for endosseous dental implant material [2]. Besides Ti, some Ti alloys are also used for dental applications, such as NiTi. The alloy NiTi is used for castings of crowns and denture construction, orthodontic archwires and brackets [25, 26]. Recently it has been found that the properties of Ti implants can be improved by using nanostructured Ti consisting of Ti-NPs [27].

Even though Ti based implants are considered to be biocompatible, their induced side effects such as hypersensitivity and allergic reactions have been reported [20, 21, 28]. These side effects might have been caused by the interaction between tissues and implants [29, 30]. The released Ti ions and Ti particles can be transported and circulated in human bodies, and might also cause cytotoxic and genotoxic effects. The release of Ni ions from NiTi alloy also has been reported [26]. Previous studies indicated that Ti ions and Ni ions induced Cytotoxicity/DNA damage in human cells [31, 32]. Ti-particles/debris (0.5-250 µm) were found in the peri-implant animal tissues after the application of Ti based implants [7, 15]. The toxic effects of Ti-particles have also been reported in previous literature: phagocytosis of Ti-particles could induce cytotoxicity in rat calvarial osteoblasts and MG63 cells [33, 34]; Ti-particles also caused genotoxic effects, which induced apoptosis in mesenchym stem cells [35, 36].

It was found that the toxicity of particles is related to the particle size and cellular uptake efficiency. The size-dependent toxicity of particles has been studied and conflicting results were found regarding the influence of the size of the particles on toxicity: nanoparticles, such as CuO-NPs and ZnO-NPs, induced higher cytotoxicity and genotoxicity than particles in micrometer size [37, 38]. In contrast to this, Fe_2O_3- , Fe_3O_4- and TiO_2-NPs were found to be not more toxic than their corresponding micrometer-sized particles [37]. The ability of different particles to enter cells may also affect the toxicity [37-39], and the particle size can impact the cellular uptake efficiency and pathway [40].

Previous study indicated that cellular uptake efficiency of silica and gold nanoparticles was size-dependent [41, 42]. However, there is less data about the toxicity and cellular uptake efficiency for Ti particles with different size available. Since Ti particles can be released to human body from Ti-based implants, it would be of great sifnificance to find out the toxicity and cellular uptake of Ti particles in relation to particle size.

In order to compare the toxicity and cellular uptake of nanometre-sized Ti, micrometre-sized Ti and NiTi particles, which can be released from dental implants or replacements, Ti-NPs (Ti 98.5%, <100 nm), Ti-MPs (Ti 99%, <44 µm) and NiTi-MPs (Ni 30%, Ti 70%, < 44 µm) were investigated. The cytotoxicity, genotoxicity and cellular uptake efficiency of these investigated particles have been measured in PDL-hTERT cells.

This work was published as follows: He X, Hartlieb E, Rothmund L, Waschke J, Wu X, Van Landuyt KL, Milz S, Michalke B, Hickel R, Reichl FX, Högg C. *Intracellular uptake and toxicity of three different Titanium particles.* Dent Mater. 2015 Jun; 31(6):734-44.

2 Materials and methods

2.1 Analysis of Ti and other metals in human jawbones with dental implants

2.1.1 Materials

The test group contained 7 samples from four human subjects with dental implants. The control group contained 6 bone samples from similar topographical regions from six human subjects without dental implants.

Samples from human subjects I-III (samples 1-6) in the test group and all the samples in control group were obtained during the dissection course of the anatomical institute of Ludwig-Maximilian-University Munich. Sample from subject IV (sample 7) in test group was supplied by the institute of forensic medicine of Ludwig-Maximilian-University Munich.

2.1.2 Sample analysis by ICP-OES

2.1.2.1 Sample preparation

All the samples had been fixed in 4% buffered formalin (Merck, Darmstadt, Germany). The soft tissue was cautiously removed and then immersed in 100% methanol.

Test group

Jawbone slices were prepared from samples 1-7 with a diamond band saw (cut-grinder macro, patho-service GmbH, Oststeinbek, Germany). The samples were cut at intervals of 1 mm in a direction toward the implants, and cutting was stopped immediately adjacent to the implants. For analysis 5 jawbone slices closest to the implant were used.

Each jawbone slice was further divided into 4 quadrants (A-D). Each quadrant was weighed and dissolved in 1 ml sub-boiled distilled nitric acid at 170ºC for 12 hours. The solution was subsequently diluted (1:5) and the contents of the elements Ti, Al, Cd, Cr, Co, Cu, Fe, Mn, Mo, Ni and V in each quadrant were analysed by ICP-OES (Optima 7300 DV, Perkin Elmer, Rodgau-Jügesheim, Germany).

Control group

Control samples were taken from mandibular regions topographically comparable to those bearing the implants. For analysis by ICP-OES, same procedure as described for sample 1-7 was performed.

2.1.2.2 Analytical procedure

Routinely after every ten measurements, three blank determinations and a control determination of a certified standard for all mentioned elements were performed. Calculation of results was carried out by relating the sample measurements to calibration curves, blank determinations, control standards and the weight of the digested sample.

2.1.3 Spatial distribution measured by LA-ICP-MS

2.1.3.1 Sample preparation

The remaining parts of samples 4-7 (with higher Ti content compated to control) and control group were dehydrated in ascending ethanol fractions, defatted in xylenes (Merk, Darmstadt, Germany) and embedded in methylmethacrylate (Fluka, Switzerland).

The polymerized methacrylate blocks were cut at a thickness of approximately 300 µm by a Leica SP 1600 saw-microtome (Leica, Wetzlar, Germany).

The distribution of the isotopes ^{47}Ti, ^{27}Al, ^{43}Ca, ^{52}Cr, ^{59}Co, ^{63}Cu, ^{57}Fe, ^{39}K, ^{55}Mn, ^{60}Ni, ^{51}V, ^{64}Zn and ^{66}Zn in each section was analysed by LA-ICP-MS-NWR-213® (New Wave Research Co. Ltd.) coupled to a NexION® 300 ICP-MS (PerkinElmer).

2.1.3.2 Analytical procedure

The laser ablations started from the bone region around 5mm from the implant and ended in the implant region.

After the laser ablations, contact radiographs (Faxitron Xray Corporation, Lincolnshire, IL, USA) for each section were taken on Agfa Strukturix x-ray sensitive film (Agfa-Gevaert, Mortsel, Belgium). The laser lines were photographed with an Axiophot microscope (Zeiss, Goettingen, Germany), equipped with Zeiss Plan-Neofluar objectives (5× and 10×) in transmitted light mode.

2.1.4 Histological analysis

2.1.4.1 Sample preparation

From each of the samples 4-7, one of the sections was glued (Cyanolit 201, Panacol LTD., Zürich, Switzerland) on opaque plastic slides, ground thinner, polished and stained with Giemsa-Eosin stain (Sigma Aldrich, Steinheim, Germany). The same procedure was applied for the control samples.

2.1.4.2 Light microscopy observation and SEM-EDX measurements

The stained sections were examined with an Axiophot microscope (Zeiss, Goettingen, Germany) that was equipped with Zeiss Plan-Neofluar objectives in transmitted light mode.

The sections that contained visible dark particles were investigated with a SEM (EVO MA 15) (Zeiss, Goettingen, Germany) equipped with secondary electron (SE) and back-scattered

electron (BSE) detectors. The EDX analyses were performed using an Oxford INCA Penta Fetx (Oxford Instruments, England).
The samples in control group were also histologically investigated and analysed by SEM-EDX.

2.2 Intracellular uptake and toxicity of three different Ti particles

2.2.1 Particle size measurement

Fresh stock solutions of Ti-MPs (Alfa Aesar, Karlsruhe, Germany), NiTi-MPs (Alfa Aesar, Karlsruhe, Germany) and Ti-NPs (Sigma–Aldrich, St. Louis, USA) were prepared by adding investigated particles (1000 mg Ti-MPs, 150 mg NiTi-MPs and 21.8 mg Ti-NPs) into 3 ml of medium and mixed. The particle size determination was performed with SEM LEO 1550 (Zeiss, Oberkochen, Germany).

2.2.2 Cytotoxicity

By using XTT-based cell viability assay the EC_{50} values for the investigated particles were determined in PDL-hTERT cells. In this assay, 20000 cells/well were incubated for 24 h and treated with different concentrations of Ti-NPs, Ti-MPs and NiTi-MPs. Negative control and positive control cells received medium and 1% Triton X-100, respectively. After exposure with investigated particles for 24 h, 50 µl of the mixture of XTT labelling reagent and electron-coupling reagent in PBS was added into the cells as described by the manufacturer (cell proliferation kit II; Roche Diagnostics GmbH Penzberg, Germany) 4 h before photometric analysis.
The cell viability was also measured by Trypan blue exclusion test. The cells were firstly treated with different concentrations of investigated particles for 24 h and then washed three times with PBS. Afterwards, the cells were detached and stained with 0.4% trypan blue (Sigma Aldrich, Steinheim, Germany) for 3 minutes. Ratio of dead cells in 100-120 cells was counted.

2.2.3 DNA damage

DNA damage of investigated particles was analysed by the alkaline single-cell microgel electrophoresis (comet assay) in red light.
PDL-hTERT cells ($2x10^5$) were incubated in 1 ml medium for 24 h. Afterwards, the cells were exposed to different concentrations of investigated particles for 24 h. Then the cells were embedded in 75 µl LMP-Agarose (Sigma Aldrich, Steinheim, Germany) on the pre-coated slide. The slide was then kept at 4 °C for at least 5 minutes, and another layer of

agarose was over stacked. After incubation at 4°C for 5 minutes, the covering glass was removed and the slide was stored in lysis buffer overnight.
Before electrophoresis, the slides were placed in the alkaline electrophoresis solution (6°C) for 30 minutes. Electrophoresis was conducted at 6°C with 25 V, maximum 300 mA for 30 minutes. The slides were then washed, stained with 200 µg/ml ethidium bromides (Sigma–Aldrich, St. Louis, USA) and evaluated using an Olympus BX 60 fluorescence microscopy (Olympus, Hamburg, Germany) with a 40x objective. OTM was applied to evaluate DNA damage [43, 44].

2.2.4 Cellular uptake

Cellular uptake of Ti-NPs, Ti-MPs and NiTi-MPs in PDL-hTERT cells was determined with LSM 510 (Zeiss, Oberkochen, Germany). The cells were incubated for 24 h on a covering glass and then exposed to Ti-NPs, NiTi-MPs and Ti-MPs at different concentrations for another 24 h. After that, the cells were stained with 2.5 µg/ml of Cell Mask Membrane Plasma Orange (Invitrogen, Oregon, USA). The cells were then fixed with 2% paraformaldehyde (Carl Roth, Karlsruhe, Germany) and stained with Sybr green I (1:50000) (Invitrogen, Oregon, USA). The covering glasses were mounted on microscopic slides using prolong gold anti-fade reagent with 4′, 6-diamidin-2-phenylindol (Invitrogen, Oregon, USA) and observed by LSM 510.
TEM Libra 120 (Zeiss, Oberkochen, Germany) was used to confirm the cellular uptake of Ti-NPs. Cells were treated with Ti-NPs (28 µg/ml) for 24 h, washed and fixed with 2% glutaraldehyde. The fixed cells were washed and then treated with 1% osmium tetroxide (Merck, Darmstadt, Germany). Dehydration was performed with ascending concentrations of ethanol: 30%, 50%, 70%, 90% and 100%. Afterwards, cells were embedded in epon 812 (Serva, Heidelberg, Germany), after the resin blocks were hardened, they were cut into ultra-thin sections (70-90 nm) with an ultra-microtome (Zeiss, Oberkochen, Germany), contrasted with 2% uranyl acetate followed by Pb-citrate and analysed by TEM Libra 120.

3 Results

3.1 Analysis of Ti and other metals in human jawbones with dental implants

3.1.1 Sample analysis by ICP-OES

Among all the investigated elements (Ti, Al, Cd, Cr, Co, Cu, Fe, Mn, Mo, Ni and V), only the element Ti in the test group (samples 1-7) showed significantly higher content compared to the control group ($p<0.05$).
The highest Ti content (13205 µg/kg-bone weight) of all total slices was detected in sample 6. The average Ti content across all 35 bone slices (n=35) of samples 1-7 (1940 ± 469 µg/kg-

bone weight) was significantly higher compared to the average content across the 30 bone slices (n=30) from the control group (634±58 µg/kg-bone weight).

There were no significant differences in Ti content averages between slices obtained at different distances from the implants. The Ti content of B quadrants (4510±1345 µg/kg-bone weight) was significantly higher compared to C (721±165 µg/kg-bone weight) and D (605±98 µg/kg-bone weight) quadrants. Quadrant B in slice 2 of sample 6 showed the highest Ti content (37700 µg/kg-bone weight) compared to all the other single quadrants.

The sum of the average Ti contents in the upper half of the bone slice - quadrants A+B (7064±1932 µg/kg-bone weight) - is significantly higher compared to the sum of the average Ti contents in the lower half of bone slice - quadrants C+D (1327±256 µg/kg-bone weight). Within the control group there were no significant differences of the Ti contents calculated for all combinations of quadrants or slices.

3.1.2 Distribution of isotopes measured by LA-ICP-MS

The isotopes ^{47}Ti, ^{27}Al, ^{43}Ca, ^{52}Cr, ^{59}Co, ^{63}Cu, ^{57}Fe, ^{39}K, ^{55}Mn, ^{60}Ni, ^{51}V, ^{64}Zn and ^{66}Zn in the bone slices with longitudinal cuts through the implants of samples 4-7 (which showed higher Ti content compared to control group measured by ICP-OES) were detected by LA-ICP-MS. ^{47}Ti was the only isotope of all investigated isotopes that could be detected in implant and human jawbone/jawbone marrow tissue of samples 4-7 (with implant) but not in the control samples without implants.

For samples 4-7 along the ablation lines different intensities of ^{47}Ti were detected. In sample 4 the distribution of ^{47}Ti along one ablation line showed that the average ^{47}Ti intensity in a bone region within about 966 µm from the implant is 14 times higher compared to average value of bone at a distance >966 µm from the implant. Samples 5-7 also showed comparable results for ^{47}Ti: increased intensities of ^{47}Ti were also detected at distances of 556 -1587 µm to the implant surfaces. ^{47}Ti can not only be found in the bone marrow tissues but also in the bone near the implant.

3.1.3 Histological analyses

The histological analysis was performed for samples 4-7 and the control group.

Observation of samples 4-7 by light microscopy revealed black dots in the bone marrow tissues, which were identified as Ti particles by SEM-EDX analysis. Primary location of Ti particles was in the bone marrow tissue at a distance of 60-700 µm from the implant, with particle sizes < 40 µm. Multinucleated cells were found in the bone marrow tissues near implant. Our result also reveals traces of bone marrow fibrosis, an indication of previous inflammatory reactions. No Ti particles, no signs of fibrosis and no multinucleated cells were found in the control group.

SEM-EDX images showed that the particle size range of Ti particles is 0.5-5 µm (detection limitation of SEM for magnification factor used in present method is 0.5 µm). The result details for this section is shown in the first publication (7.1.1).

3.2 Intracellular uptake and toxicity of three different Ti particles

3.2.1 Particle size measurement

About 90% of Ti-NPs were sized below 100 nm and 0.6% of Ti-NPs were sized above 200 nm. Ti-MPs were sized between 0.3 µm and 43 µm; about 12% of Ti-MPs were below 1 µm, more than 50% of the particles were sized below 5 µm. NiTi-MPs were sized between 0.7 µm and 90 µm, 60% of the particles were sized above 10 µm and 17% of small particles were sized below 5 µm, only 4% of the small particles were below 1 µm.

3.2.2 Cytotoxicity

3.2.2.1 XTT viability assay

Ti-NPs showed the highest toxic potential with an EC_{50} of 2.84±0.37 mg/ml (mean±SD, n=4). EC_{50} value of NiTi was 41.8±4 mg/ml (mean±SD, n=4). EC_{50} value for Ti-MPs could not be determined at the concentration <999 mg/ml and no higher concentrations of Ti-MPs were investigated.

3.2.2.2 Cell death

Ti-NPs caused 9% and 19% increase in cell death at the concentration of 284 µg/ml (1/10 EC_{50}, $p<0.01$) and 1420 µg/ml (1/2 EC_{50}, $p<0.001$), compared to the medium (including 6% of dead cells). No significant difference for Ti-NPs was detected at the lower concentrations 1/50 and 1/100 EC_{50}, compared to medium.

NiTi-MPs induced 9% more cell death ($p<0.01$) at the concentration of 20900 µg/ml (1/2 EC_{50}) compared to medium. No significant difference was found at 1/10 EC_{50}, 1/50 EC_{50} and 1/100 EC_{50}.

Ti-MPs only caused 9% increase ($p<0.05$) of dead cells at the highest concentration (33300 µg/ml), compared to medium. No significant difference was found at lower concentrations.

3.2.3 DNA damage

After Ti-NPs exposure at all investigated concentrations, a significant increase in OTM value (compared to negative control) was detected ($p<0.01$). The mean OTM value for Ti-NPs at 1/10 EC_{50} was significantly higher compared to 1/50 EC_{50}, 1/100 EC_{50} and 1/200 EC_{50} ($p<0.01$). There is no significant difference detected among 1/50 EC_{50}, 1/100 EC_{50}, and 1/200 EC_{50}. A significant increase in OTM value ($p<0.001$) was observed at the concentration of 4180 µg/ml (1/10 EC_{50}) after NiTi-MPs exposure compared to negative control. Ti-MPs induced a significant increase in OTM value ($p<0.001$) at the concentration

of 6666 µg/ml but no significant difference at the lower concentrations (3333 µg/ml, 666 µg/ml and 333 µg/ml).
In addition, the OTM value of Ti-NPs at the concentration of 284 µg/ml (1/10 EC_{50}) was 1.5 times higher than OTM value of NiTi-MPs at the concentration of 4180 µg/ml (1/10 EC_{50}). 284 µg/ml (1/10 EC_{50}) of Ti-NPs induced a significantly higher OTM value compared to Ti-MPs at 6666 µg/ml ($p<0.001$).

3.2.4 Cellular uptake

Ti-NPs could be detected in the cytoplasm and nucleus of PDL-hTERT cells, while for NiTi-MPs and Ti-MPs, no particles were detected in the nucleus, particles around 1 µm were found in the PDL-hTERT cytoplasm. The ratio of cells with Ti-NPs inside the cytoplasm significantly increased ($p<0.05$) when the exposure concentration of Ti-NPs was raised. The ratio of cells with Ti-NPs in the nucleus also increased significantly from 5.0±1.5% (mean ±SD, n=4) to 11%±1.3% (mean ± SD, n=4) when the exposure concentration was increased. For NiTi-MPs, no significant difference was found in the cellular uptake efficiency when the exposure concentration increased from 418 to 4180 µg/ml. For Ti-MPs (418 µg/ml), 33%±4.5% (mean ± SD, n=4) of the detected cells were found with Ti-MPs in the cytoplasm. The cellular uptake of Ti-NPs in PDL-hTERT cells was confirmed with TEM. After exposure to 28 µg/ml (1/10 EC_{50}) of Ti-NPs for 24 h, particles between 30 nm and 200 nm were detected inside the cytoplasm.

4 Synopsis/ Zusammenfassung

4.1 Synopsis

In recent years, Ti is commonly used for dental implants [6] due to its high corrosion resistance, high biocompatibility, high strength and light weight. However, the animal studies indicated that Ti implant can release debris including particles and ions into the surrounding bone or bone marrow tissues [7, 15-17]. The released Ti species can even be circulated in blood and lymph [12, 18, 19]. Possible side effects (including bone marrow fibrosis, necrosis and allergic reactions) relating to Ti implants were also reported [20-23]. Therefore, it would be of great significance to find out whether the Ti-implants can induce health problems to human beings and how the Ti-implant causes the health problems.
In the first study, Ti content released from dental implants in the human jawbones was measured, which can be taken as a reference for the risk assessment of Ti-implants in human. In this study, the level of released Ti from dental implants was determined by ICP-OES, the distribution of Ti in human jawbone or bone marrow tissues was measured with LA-ICP-MS, and the particles detached from dental implants were observed and identified with

light microscopy and SEM-EDX. The effect of released Ti particles on human tissues was also investigated with histological analysis.

In the second study, the toxicity and cellular uptake of three kinds of Ti particles (NiTi-MPs, Ti-MPs and Ti-NPs) in PDL-hTERT cells were investigated. The toxicity of these Ti particles was measured by using XTT test and comet assay. Morever, the cellular uptake of the investigated particles in PDL-hTERT cells was also detected by LSCM and TEM, and with these results the ability of investigated particles to enter PDL-hTERT cells was investigated.

By comparing the released Ti content detected in the first study and the EC_{50} of three investigated particles determined in the second study, a rough risk assessment was conducted. In the first study, Ti particles (0.5-5 µm) detached from dental implants were observed in the bone marrow tissues, and in the second study the cellular uptake of Ti particles with different sizes was determined, which might give a clue for the toxicity and transportation of Ti particles in human bone/ bone marrow tissues.

4.1.1 Analysis of Ti and other metals in human jawbones with dental implants

4.1.1.1 ICP-OES

Among the analysed elements, only Ti showed significantly higher contents in the test group compared to the control group. The highest content detected in the test group was 37700 µg/kg-bone weight. Our human jawbones were obtained from the forensic medicine and the anatomical insititution of LMU Munich. Due to ethical considerations, it is not possible to give the detail information about these implants in test group, such as the “age” of the implants, the type of the implants, the method of surgeon and surface treatment of the implants and impurities present in the implant before insertion. But what we can be sure is that Ti implants can really release Ti species into the human bone, and among 35 slices from 7 samples in the test group, the highest Ti content is 37700 µg/kg-bone weight.

4.1.1.2 LA-ICP-MS

The distributions of 13 isotopes ^{47}Ti, ^{27}Al, ^{43}Ca, ^{52}Cr, ^{59}Co, ^{63}Cu, ^{57}Fe, ^{39}K, ^{55}Mn, ^{60}Ni, ^{51}V, ^{64}Zn and ^{66}Zn in bone samples 4-7 with implants were measured by LA-ICP-MS. In bone samples without implant no increased ^{47}Ti was detected. Increased intensity of ^{47}Ti for samples 4-7 was detected in the bone region adjacent to the implant (about 556-1587 µm away from the implant surface). And this indicated that Ti can migrate from the implant into the surrounding human jawbone or jawbone marrow tissues. In addition, the intensity of ^{47}Ti increased with decreasing distance from the implants, which suggests that the distribution of ^{47}Ti in the jawbone depends on the distance from the implant. Interestingly, ^{47}Ti is present not only in the peri-implant human jawbone marrow tissues but also in the cortical or trabecular bone matrix adjacent to the implant.

4.1.1.3 Histological analyses

In the current study, SEM results showed Ti particles with a size of 0.5-5 µm in human jawbone marrow tissues. Clinical studies indicated that particles of Ti and Ti alloys ranging from 0.01 µm (10 nm) to 50 µm can be released into human body from Ti-based implants or replacements [19, 45] and the animal studies demonstrated the presence of Ti particles/debris sized between 3 µm and 250 µm in the peri-implant bone or tissues [7, 15]. The particle sizes of our investigated particles are in these reported ranges. Previous studies reported that particles <1 µm could be taken up by non-phagocytic eukaryotic cells via endocytosis [46] and particles with diameters exceeding 0.75 µm can be taken up by macrophages, neutrophils and monocytes via phagocytosis or through macropinocytosis (>1 µm) by all cell types [47]. Therefore, transportation of Ti particles with size of 0.5-5 µm observed in human bone marrow tissues of present study into cells is possible.

Bone marrow fibrosis and multinucleated cells were observed near the implant in this study. Similarly, a previous post-mortem study about metal particles released from implants showed fibrosis in lymph-node [22]. Furthermore, multinucleated cells have been observed after hydroxyapatite implantation in rat periodontal tissues [48]. Bone marrow fibrosis might be induced by marrow injury and inflammation [49]. These effects are reported to be associated with surgical trauma during insertion of implants [50]. Multinucleated giant cells can be elicited by wear particles in periprosthetic tissues in human specimens and these cells might contain phagocytized wear particles [51]. Therefore, the observed bone marrow fibrosis and multinucleated giant cells might be associated with the dental implants.

4.1.2 Intracellular uptake and toxicity of three different Ti particles

In this study, the toxic potential of Ti-NPs, Ti-MPs and NiTi-MPs in PDL-hTERT cells was measured and compared according to their particle size and cellular uptake efficiency.

4.1.2.1 Cytotoxicity: XTT assay and cell death

It is previously reported that the cytotoxicity of NPs might have been induced by their large surface area per mass, release of toxic ions and ability to pass the cell membrane [38, 52]. In the present study, XTT test and trypan blue exclusion test were used to measure the cytotoxicity of Ti-NPs, Ti-MPs and NiTi-MPs in PDL-hTERT cells. The results of XTT test indicated that Ti-NPs induced higher cytotoxicity than Ti-MPs, which is also confirmed by the trypan blue exclusion test.

Previous studies showed that Ti particles sized below 150 µm exhibited no cytotoxicity in human fibroblasts [53, 54], but 10 µg/ml of TiO_2-NPs with a size of 30 nm could induce 40% reductions in the cell viabilities of human amnion epithelial cells [54]. In addition, our results indicated that the EC_{50} of Ti-MPs (<44 µm) in PDL-hTERT cells was above 999 mg/ml, while the EC_{50} of Ti-NPs with size between 20 nm and 250 nm was 2.84 mg/ml [55]. Regarding the highest Ti content (37700 µg/kg) detected in the human bones, a following calculation for a rough risk assessment was conducted: assuming that Ti in 1 kg bone corresponds to Ti in 1

L fluid, a maximal Ti concentration of 38 µg/ml can be calculated. Assuming it contains only Ti-NPs in this concentration, and we found that this value (38 µg/ml) is 74 times lower compared to the EC_{50} (2.84 mg/ml) of Ti NPs [55].

4.1.2.2 DNA damage

Comet assay was performed to determine the DNA damage caused by investigated Ti particles, which indicated that 14 µg/ml of Ti-NPs induced around 1.5-fold increase in OTM value compared to negative control in PDL-hTERT cells; while a 500 fold concentration (6666 µg/ml) was required for Ti-MPs to get the same extent of DNA damage with Ti-NPs. The increase in OTM value is considered to be an indicator of DNA damage [43, 44]; therefore, Ti-NPs displayed a 500-time higher DNA damage potential compared to Ti-MPs. On the contrary, in previous studies Fe_2O_3-NPs and TiO_2-NPs caused significantly ($p<0.05$) less DNA damage (5% less in tail) compared to the corresponding MPs at the same concentrations [37]. But it was also described that NPs of ZnO and CuO, induced more DNA damage than their corresponding MPs: ZnO-NPs induced a significant increase in DNA damage in human nasal mucosa cells starting from the concentration of 10 µg/ml ($p<0.05$), in comparison to the negative control, while no DNA damage was observed with ZnO-MPs at the same concentration [38]; a 4-h exposure to CuO-NPs induced 4 times more DNA damage in A549 cells at the concentration of 40 µg/cm^2 compared to the control group, same concentration of CuO-MPs only caused 0.5 fold more DNA damage [37].

4.1.2.3 Cellular uptake

Ti-NPs showed the highest cellular uptake efficiency but with smaller particle size, compared to Ti-MPs and NiTi-MPs, which indicates that the uptake of Ti particles in PDL-hTERT cells is also size-dependent. This result for Ti-NPs is in line with previous studies. These former studies reported that non-phagocytic eukaryotic cells could take up particles that are below 1 µm [46], and the cellular uptake efficiency of nanoparticles can be affected by particle size [41, 42, 56]: smaller particles (in nanometre) could mediate higher cellular uptake than big particles in micrometre size.

In the present study, in addition to the detected highest cellular uptake efficiency, the highest cytotoxicity was also determined for Ti-NPs, compared to Ti-MPs and NiTi-MPs. Similar result has been reported by a previous study, where toxicity of SiTi-NPs in macrophages has been correlated to the cellular uptake efficiency: cationic SiTi-NPs (50 nm) induced the highest uptake efficiency and also the most toxic effects (e.g. cytotoxicity) on macrophages J774A.1 cells compared to the other SiTi-NPs with different sizes and coating surfaces[39]. Therefore, our results indicated that the cellular uptake of Ti particles might correlate with the toxic effects on the cells, and a higher cellular uptake can cause more toxic effects. Furthermore, the results of the present study showed that only Ti-NPs were found in the nucleus and Ti-NPs induced more DNA damage compared to Ti-MPs and NiTi-

MPs. So the higher potential of DNA damage for NPs might also be explained by the nuclear uptake of NPs.

Conclusions:

In this study, the highest content of Ti released from dental implants in human jawbones is 37700 µg/kg-bone weight, which is more than 70 times lower than the EC_{50} of Ti-NPs in human PDL-hTERT cells. Ti particles in size between 0.5 µm and 40 µm were observed in the jawbone marrow tissues near the implant, which might induce fibrosis and multinucleated cells in bone marrow tissues.

Ti-NPs which have small particle size could induce higher cellular uptake and higher toxic effects compared to the other Ti particles. Therefore, it is suggested that the cellular uptake of Ti particles might induce toxic effects on human cells. According to the "worst case situation" risk assessment results, we suggest that Ti dental implants might have no adverse effects in clinical use. However, our study on human jawbones also indicated that the released Ti from dental implants is not totally inert.

4.2 Zusammenfassung

In letzter Zeit war Ti wegen seiner hohen Korrosionsfestigkeit, seiner hohen Biokompatibilität, seiner hohen Stabilität und seinem geringen Gewicht ein gebräuchliches Material für Zahnimplantate [6]. Jedoch zeigten Tierversuche das Ti-Implantate Fremdstoffe wie Partikel und Ionen in den umgebenden Knochen oder Knochenmark freisetzen können [7, 15-17]. Freigesetztes Titan kann sogar in Blut und Lymphe zirkulieren [12, 18, 19]. Über mögliche Nebenwirkungen in Verbindung mit Ti-Implantaten (Z.B. Knochenmarkfibrose, Nekrose und allergische Reaktionen) wurde berichtet [20-23]. Darum ist es von großer Bedeutung, herauszufinden ob Ti-Implantate Gesundheitsprobleme beim Menschen verursachen und wie das Ti-Implantat diese Probleme verursacht.

In der ersten Studie wurde die vom Implantat im menschlichen Kieferknochen freigesetzte Menge an Titan gemessen, was als Grundlage für eine Risikobewertung von Ti-Implantaten im Menschen genutzt werden kann. Der Ti-Gehalt wurde mit ICP-OES, die Ti-Verteilung im humanen Kieferknochen und Knochenmark wurde mit LA-ICP-MS bestimmt. Die vom Implantat losgelösten Partikel wurden detektiert und identifiziert mit Lichtmikroskopie und SEM-EDX. Die Auswirkungen der freigesetzten Ti-Partikel auf das menschliche Gewebe wurden histologisch untersucht.

In der Zweiten Studie wurden drei Arten von Ti-Partikeln (NiTi-MPs, Ti-MPs und Ti-NPs) an PDL-hTERT Zellen auf die Toxizität und die zelluläre Aufnahme untersucht. Die Toxizität der Partikel wurde mit dem XTT-Test und dem Comet Assay gemessen, die zelluläre

Partikelaufnahme wurde mit LSCM und TEM bestimmt und mit diesen Ergebnissen die Fähigkeit der Partikel zum Eindringen in PDL-hTERT Zellen untersucht.
Durch Vergleich der freigesetzten Ti-Menge aus Studie eins mit den EC_{50}-Werten der drei untersuchten Partikelarten aus Studie zwei wurde eine Risikoabschätzung erstellt. In der ersten Studie wurden vom Implantat losgelöste Ti-Partikel (0,5-5 µm) im Knochenmark festgestellt und in der zweiten Studie wurde die zelluläre Aufnahme von Ti-Partikel mit unterschiedlicher Größe bestimmt was schlussfolgern lässt auf die Toxizität und den Transport von Ti-Partikel im humanen Knochen und Knochenmark.

4.2.1 Analyse von Ti und anderen Metallen im menschlichen Kieferknochen mit Dentalimplantaten

4.2.1.1 ICP-OES

Unter den analysierten Elementen zeigte nur Ti signifikant höhere Gehalte beim Vergleich der Testgruppe mit der Kontrollgruppe. Der höchste Gehalt in der Testgruppe war 37700 µg/kg Knochengewicht. Die Proben wurden aus der Rechtsmedizin und der Anatomie der LMU München gewonnen. Wegen der ethischen Gesetzgebung ist es nicht möglich, detaillierte Informationen zu den Implantaten der Testgruppe zu geben, wie das “Alter” der Implantate, der Typ des Implantats, die Methode der Implantation, die Oberflächenbehandlung des Implantats und die schon vor der Implantation im Titankörper vorhandenen Verunreinigungen. Ti-Implantate können Ti-Verbindungen im menschlichen Knochen deponieren. Unter den 35 Knochenscheiben von sieben Knochenproben war in der Testgruppe der höchste Ti-Gehalt mit 37700 µg/kg Knochengewicht zu finden.

4.2.1.2 LA-ICP-MS

Die Verteilung von 13 Isotopen (^{47}Ti, ^{27}Al, ^{43}Ca, ^{52}Cr, ^{59}Co, ^{63}Cu, ^{57}Fe, ^{39}K, ^{55}Mn, ^{60}Ni, ^{51}V, ^{64}Zn und ^{66}Zn) in den Knochenproben 4-7 mit Implantat wurde mittels LA-ICP-MS gemessen. In Knochenproben ohne Implantat wurden keine erhöhten ^{47}Ti Gehalte gemessen. Erhöhte ^{47}Ti Intensitäten wurde bei den Proben 4-7 im Implantat naheliegenden Regionen (zwischen 556-1587 µm entfernt von der Implantat Oberfläche) gemessen. Dies zeigt, dass Ti vom Implantat in den umgebenden Kieferknochen oder sogar in das Kieferknochenmark wandern kann. Die Intensität von ^{47}Ti steigt an mit abnehmender Distanz zum Implantat und zeigt, dass die Verteilung von ^{47}Ti im Kieferknochen von der Distanz zum Implantat abhängt. ^{47}Ti befindet sich nicht nur im Implantat nahem humanen Kieferknochenmark, sondern auch in der das Implantat umgebenden kortikalen und trabekularen Knochenmatrix.

4.2.1.3 Histologische Untersuchungen

In der vorliegenden Studie zeigten SEM-Aufnahmen Ti-Partikel mit einer Größe von 0,5-5 µm im humanen Kieferknochenmark. Klinische Studien zeigten, dass Partikel aus Ti und Ti-Legierungen in der Größe von 0,01 µm (10 nm) bis zu 50 µm im menschlichen Körper von Ti-basierten Implantaten und Prothesen freigesetzt werden können [19, 45] und Tierversuche

lieferten den Nachweis von Ti-Partikeln und –Überresten in der Größe zwischen 3 µm und 250 µm im Implantat nahen Knochen oder Gewebe [7, 15]. Die von uns untersuchten Partikel lagen innerhalb dieses Größenbereichs. Vorhergehende Studien zeigten, dass Partikel <1 µm von nicht phagozytierenden eukaryotischen Zellen per Endozytose aufgenommen können [46] und Partikel deren Durchmesser 0,75 µm überschritten von Makrophagen, Neutrophilen und Monozyten durch Phagozytose, oder durch Makropinozytose (>1 µm) von allen Zelltypen aufgenommen werden [47]. Deshalb ist der Transport von Ti-Partikel mit einer Größe von 0,5-5 µm ins Zellinnere möglich, so wie auch in der vorliegenden Studie im humanen Knochenmark beobachtet wurde.

Knochenmarkfibrose und mehrkernige Riesenzellen nahe dem Implantat wurden in dieser Studie festgestellt. Ebenso zeigte eine vorhergehende post mortem Studie über von Implantaten freigesetzten Metallpartikel, Fibrosen in Lymphknotengewebe [22]. Weiterhin wurden mehrkernige Riesenzellen in periodontalen Rattengewebe beobachtet nach Implantierung von Hydroxyapatit [48]. Knochenmarkfibrose kann von Knochenmark-verletzungen und Entzündungen verursacht werden [49]. Diese Auswirkungen wurden in Zusammenhang mit chirurgischen Traumata während des Einsetzens von Implantaten festgestellt [50]. Mehrkernige Riesenzellen können im prothesennahen humanen Gewebe von eingetragenen Partikeln aufnehmen und diese Zellen können phagozytierte Partikel enthalten [51]. Darum können die beobachteten Knochenmarkfibrosen und mehrkernige Riesenzellen in Zusammenhang mit den Zahnimplantaten stehen.

4.2.2 Intrazelluläre Aufnahme und Toxizität von drei verschiedenen Ti partikelarten

In dieser Studie wurde das toxische Potential von Ti-NPs, Ti-MPs und NiTi-MPs in PDL-hTERT Zellen gemessen und in Hinblick auf ihre Partikelgröße und zellulare Aufnahmeeffizienz verglichen.

4.2.2.1 Zytotoxizität: XTT-Versuch und Zelltod

Es wurde bereits veröffentlicht, dass die Zytotoxizität von Nanopartikeln von der großen Oberfläche im Verhältnis zur Masse, beim Freisetzen toxischer Ionen und von ihrer Fähigkeit die Zellmembran zu passieren, hervorgerufen werden kann [38, 52]. In der vorliegenden Studie wurde der XTT-Test und der Trypanblau Farbausschlusstest benutzt um die Zytotoxizität von Ti-NPs, Ti-MPs und NiTi-MPs in PDL-hTERT Zellen zu messen. Die Ergebnisse des XTT-Tests ergaben, dass Ti-NPs eine höhere Toxizität verursachen als Ti-MPs, was auch durch den Trypanblau Farbausschlusstest bestätigt wurde.

Frühere Studien zeigten, dass Ti-Partikel kleiner als 150 µm keine Zytotoxizität in menschlichen Fibroblasten generieren [53, 54], aber 10 µg/ml TiO_2 Nanopartikel mit einer Größe von 30 nm können die Zellvitalität in Amnionepithelzellen um 40% reduzieren [54]. Unsere Ergebnisse ergaben, dass die EC_{50} von Ti-MPs (<44 µm) in PDL-hTERT Zellen über 999 mg/ml lag, während die EC_{50} von Ti-NPs mit Größen zwischen 20 nm und 250 nm in der

Konzentration von 2,84 mg/ml war [55]. Unter Bezugnahme auf den höchsten im menschlichen Knochen gemessenen Ti-Gehalt (37700 µg/kg) wurde die folgende Berechnung einer groben Risikobewertung für ein "Worst Case Szenario" durchgeführt: Es wird angenommen, dass der Ti-Gehalt in 1 kg Knochen der Ti-Konzentration in einem Liter Flüssigkeit entspricht. Dies ergibt eine maximale Ti-Konzentration von 38 µg/ml. Es wird ferner angenommen, dass diese Konzentration nur Ti-NPs enthalte, so ergibt sich ein Gehalt von 38 µg/ml, der ca. 74 mal kleiner als der EC_{50}-Wert von Ti-NPs ist [55].

4.2.2.2 DNA-Schädigung

Zur Bestimmung der von Ti-Partikel verursachten DNA-Schädigung wurde der Comet-Assay durchgeführt, welcher ergab, dass 14 µg/ml Ti-NPs in PDL-hTERT Zellen einen 1,5 fachen Anstieg der OTM-Werte im Vergleich zur Negativkontrolle bewirkten, während die ca. 500-fache Konzentration (6666 µg/ml) an Ti-MPs nötig war, um das gleiche Ausmaß an DNA-Schäden zu erzeugen, wie mit den Ti-NPs. Der Anstieg der OTM-Werte ist ein Indikator für DNA-Schäden [43, 44]; So stellen Ti-NPs ein 500-fach höheres DNA-Schädigungspotential dar, verglichen mit Ti-MPs. Gegenteilig wurde in vorigen Studien gefunden, dass Fe_2O_3- und TiO_2-Nanopartikel signifikant ($p<0,05$) weniger DNA-Schäden verursachen (5% geringerer Schweif), verglichen mit den entsprechenden Makropartikel in der gleichen Konzentration [37]. Aber es wurde auch gefunden, dass Nanopartikel aus ZnO oder CuO mehr DNA-Schäden verursachten als ihre entsprechenden Makropartikel: ZnO-Nanopartikel verursachten eine signifikante Zunahme der DNA-Schäden in humanen Nasenschleimhaut-Zellen beginnend mit einer Konzentration von 10 µg/ml ($p<0,05$), im Vergleich zur Negativ-Kontrolle, während bei ZnO-Makropartikel der gleichen Konzentration keine DNA-Schäden gesehen wurden [38]. CuO-Nanopartikel (40 µg/cm^2) induzierten nach vierstündiger Exposition in humanen A549-Zellen vier Mal mehr DNA-Schäden, im vergleich zur Kontrolle, die gleiche Konzentration an CuO-Mikropartikel verursachte nur 0,5 fachen mehr DNA- Schäden [37].

4.2.2.3 Zelluläre Aufnahme

Ti-NPs erreichten die höchste zelluläre Partikelaufnahmerate. Die aufgenommenen Partikel waren allerdings kleiner, verglichen mit Ti-MPs und NiTi-MPs, was indiziert, dass die Aufnahme von Ti-Partikel in PDL-hTERT Zellen größenabhängig ist. Dieses Ergebnis für Ti-NPs bestätigt frühere Studien. Diese Studien ergaben, dass nicht phagozytierende eukaryotische Zellen Partikel kleiner als 1 µm aufnehmen können [46] und dass die zelluläre Aufnahmerate von Nanopartikel von der Partikelgröße abhängig ist [41, 42, 56]: Nanopartikel erzielten höhere Aufnahmeraten als größere Partikel im Mikrometerbereich. In der vorliegenden Studie wurde, verglichen mit Ti-MPs und NiTi-MPs, für Ti-NPs sowohl die höchste zelluläre Partikelaufnahmerate, als auch die höchste Zytotoxizität gefunden. Analoge Resultate ergab eine frühere Studie, in welcher die Toxizität von Silizium-Titan Hohlkörper (SiTi)-Nanopartikel auf Makrophagen mit der Partikelaufnahmerate korrelierte. Der Vergleich verschiedener Si-

Nanopartikel mit unterschiedlicher Größe und Oberflächenbeschichtung ergab in J774A.1 Makrophagenzellen für den gleichen Partikeltyp, die kationischen SiTi-Nanopartikel (50 nm), sowohl höchste Partikelaufnahmeraten als auch die höchsten toxischen Effekte (z.B. Zytotoxizität) [39]. Unsere Ergebnisse zeigten, dass die zelluläre Aufnahme von Ti-Partikeln einher geht mit toxischen Effekten an den Zellen. Des Weiteren zeigen die Ergebnisse, dass nur Ti-NPs im Zellkern gefunden wurden und dass Ti-NPs mehr DNA-Schäden verursachten, verglichen mit Ti-MPs und NiTi-MPs. So kann das höhere DNA-schädigende Potential von Nanopartikel durch die Aufnahme der Nanopartikel in den Zellkern erklärt werden.

Schlussfolgerungen:

Der höchste Kieferknochen-Gehalt von Ti, der aus Dentalimplantaten freigesetzt wurde, war in dieser Studie 37700 µg/kg Knochengewicht, was mehr als 70-mal geringer ist, als die EC_{50} von Ti-NPs in menschlichen PDL-hTERT Zellen. Ti-Partikel mit einer Größe zwischen 0,5 µm und 40 µm wurden nahe dem Implantat im humanen Kieferknochenmarkgewebe entdeckt, was im Knochenmark zur Bildung von vielkernigen Riesenzellen und Fibrosen führen kann.

Durch die Besonderheit ihrer geringen Partikelgröße haben Ti-NPs eine höhere zelluläre Aufnahmerate und können stärkere toxische Effekte auslösen, verglichen mit den anderen Ti-Partikeln. Deshalb könnte die zelluläre Ti-Partikelaufnahme auch toxische Effekte in humanen Zellen auslösen. Berechnungen auf das “Ti-Worst Case Szenario” in der menschlichen physiologischen Situation ergeben, dass Ti-Implantate keine negativen Auswirkungen im klinischen Einsatz darstellen. Die Ergebnisse dieser Studie indizieren jedoch, dass Ti, freigesetzt aus menschlichen Ti-Implantaten, als nicht völlig inert anzusehen ist.

5 References

[1] Lautenschlager EP, Monaghan P. Titanium and titanium alloys as dental materials. Int Dent J. 1993;43:245-53.
[2] Elias C, Lima J, Valiev R, Meyers M. Biomedical applications of titanium and its alloys. Jom. 2008;60:46-9.
[3] McCracken M. Dental implant materials: commercially pure titanium and titanium alloys. Journal of prosthodontics. 1999;8:40-3.
[4] Kasemo B. Biocompatibility of titanium implants: surface science aspects. J Prosthet Dent. 1983;49:832-7.
[5] Schliephake H, Reiss G, Urban R, Neukam FW, Guckel S. Metal release from titanium fixtures during placement in the mandible: an experimental study. Int J Oral Maxillofac Implants. 1993;8:502-11.
[6] Okabe T, Hero H. The use of titanium in dentistry. Cells and Materials(USA). 1995;5:211-30.
[7] Franchi M, Bacchelli B, Martini D, Pasquale VD, Orsini E, Ottani V, et al. Early detachment of titanium particles from various different surfaces of endosseous dental implants. Biomaterials. 2004;25:2239-46.
[8] Adya N, Alam M, Ravindranath T, Mubeen A, Saluja B. Corrosion in titanium dental implants: literature review. The Journal. 2005;5:127.
[9] Velasco-Ortega E, Jos A, Cameán AM, Pato-Mourelo J, Segura-Egea JJ. < i> In vitro</i> evaluation of cytotoxicity and genotoxicity of a commercial titanium alloy for dental implantology. Mutation Research/Genetic Toxicology and Environmental Mutagenesis. 2010;702:17-23.
[10] Meachim G, Williams D. Changes in nonosseous tissue adjacent to titanium implants. Journal of biomedical materials research. 1973;7:555-72.
[11] Galante JO, Lemons J, Spector M, Wilson PD, Jr., Wright TM. The biologic effects of implant materials. J Orthop Res. 1991;9:760-75.
[12] Hallab NJ, Mikecz K, Vermes C, Skipor A, Jacobs JJ. Orthopaedic implant related metal toxicity in terms of human lymphocyte reactivity to metal-protein complexes produced from cobalt-base and titanium-base implant alloy degradation. Molecular and cellular biochemistry. 2001;222:127-36.
[13] Hallab NJ, Jacobs JJ, Skipor A, Black J, Mikecz K, Galante JO. Systemic metal-protein binding associated with total joint replacement arthroplasty. J Biomed Mater Res. 2000;49:353-61.
[14] Jacobs JJ, Gilbert JL, Urban RM. Current Concepts Review-Corrosion of Metal Orthopaedic Implants*. The Journal of Bone & Joint Surgery. 1998;80:268-82.
[15] Martini D, Fini M, Franchi M, Pasquale VD, Bacchelli B, Gamberini M, et al. Detachment of titanium and fluorohydroxyapatite particles in unloaded endosseous implants. Biomaterials. 2003;24:1309-16.
[16] Ferguson AB, Akahoshi Y, Laing PG, Hodge ES. Characteristics of trace ions released from embedded metal implants in the rabbit. The Journal of Bone & Joint Surgery. 1962;44:323-36.
[17] Ducheyne P, Willems G, Martens M, Helsen J. In vivo metal-ion release from porous titanium-fiber material. Journal of biomedical materials research. 1984;18:293-308.
[18] Brien WW, Salvati EA, Betts F, Bullough P, Wright T, Rimnac C, et al. Metal levels in cemented total hip arthroplasty. A comparison of well-fixed and loose implants. Clin Orthop Relat Res. 1992:66-74.
[19] Urban RM, Jacobs JJ, Tomlinson MJ, Gavrilovic J, Black J, Peoc'h M. Dissemination of wear particles to the liver, spleen, and abdominal lymph nodes of patients with hip or knee replacement. J Bone Joint Surg Am. 2000;82:457-76.
[20] Sicilia A, Cuesta S, Coma G, Arregui I, Guisasola C, Ruiz E, et al. Titanium allergy in dental implant patients: a clinical study on 1500 consecutive patients. Clin Oral Implants Res. 2008;19:823-35.
[21] Lalor PA, Revell PA, Gray AB, Wright S, Railton GT, Freeman MA. Sensitivity to titanium. A cause of implant failure? J Bone Joint Surg Br. 1991;73:25-8.
[22] Case CP, Langkamer VG, James C, Palmer MR, Kemp AJ, Heap PF, et al. Widespread dissemination of metal debris from implants. J Bone Joint Surg Br. 1994;76:701-12.

[23] Amstutz HC, Campbell P, Kossovsky N, Clarke IC. Mechanism and clinical significance of wear debris-induced osteolysis. Clin Orthop Relat Res. 1992:7-18.
[24] Dannenmaier WC, Haynes DW, Nelson CL. Granulomatous reaction and cystic bony destruction associated with high wear rate in a total knee prosthesis. Clin Orthop Relat Res. 1985:224-30.
[25] Thompson SA. An overview of nickel-titanium alloys used in dentistry. Int Endod J. 2000;33:297-310.
[26] Setcos JC, Babaei-Mahani A, Silvio LD, Mjor IA, Wilson NH. The safety of nickel containing dental alloys. Dent Mater. 2006;22:1163-8.
[27] Valiev RZ, Semenova IP, Latysh VV, Rack H, Lowe TC, Petruzelka J, et al. Nanostructured titanium for biomedical applications. Advanced engineering materials. 2008;10:B15-B7.
[28] Egusa H, Ko N, Shimazu T, Yatani H. Suspected association of an allergic reaction with titanium dental implants: a clinical report. J Prosthet Dent. 2008;100:344-7.
[29] Hansen DC. Metal corrosion in the human body: the ultimate bio-corrosion scenario. The Electrochemical Society Interface. 2008;17:31.
[30] Yang J, Merritt K. Detection of antibodies against corrosion products in patients after Co-Cr total joint replacements. J Biomed Mater Res. 1994;28:1249-58.
[31] Soto-Alvaredo J, Blanco E, Bettmer J, Hevia D, Sainz RM, Lopez Chaves C, et al. Evaluation of the biological effect of Ti generated debris from metal implants: ions and nanoparticles. Metallomics. 2014;6:1702-8.
[32] Faccioni F, Franceschetti P, Cerpelloni M, Fracasso ME. In vivo study on metal release from fixed orthodontic appliances and DNA damage in oral mucosa cells. Am J Orthod Dentofacial Orthop. 2003;124:687-93; discussion 93-4.
[33] Pioletti DP, Takei H, Kwon SY, Wood D, Sung KL. The cytotoxic effect of titanium particles phagocytosed by osteoblasts. J Biomed Mater Res. 1999;46:399-407.
[34] Lohmann CH, Schwartz Z, Koster G, Jahn U, Buchhorn GH, MacDougall MJ, et al. Phagocytosis of wear debris by osteoblasts affects differentiation and local factor production in a manner dependent on particle composition. Biomaterials. 2000;21:551-61.
[35] Wang ML, Nesti LJ, Tuli R, Lazatin J, Danielson KG, Sharkey PF, et al. Titanium particles suppress expression of osteoblastic phenotype in human mesenchymal stem cells. J Orthop Res. 2002;20:1175-84.
[36] Wang ML, Tuli R, Manner PA, Sharkey PF, Hall DJ, Tuan RS. Direct and indirect induction of apoptosis in human mesenchymal stem cells in response to titanium particles. J Orthop Res. 2003;21:697-707.
[37] Karlsson HL, Gustafsson J, Cronholm P, Moller L. Size-dependent toxicity of metal oxide particles--a comparison between nano- and micrometer size. Toxicol Lett. 2009;188:112-8.
[38] Hackenberg S, Scherzed A, Technau A, Kessler M, Froelich K, Ginzkey C, et al. Cytotoxic, genotoxic and pro-inflammatory effects of zinc oxide nanoparticles in human nasal mucosa cells in vitro. Toxicol In Vitro. 2011;25:657-63.
[39] Oh WK, Kim S, Choi M, Kim C, Jeong YS, Cho BR, et al. Cellular uptake, cytotoxicity, and innate immune response of silica-titania hollow nanoparticles based on size and surface functionality. ACS nano. 2010;4:5301-13.
[40] Lee KD, Nir S, Papahadjopoulos D. Quantitative analysis of liposome-cell interactions in vitro: rate constants of binding and endocytosis with suspension and adherent J774 cells and human monocytes. Biochemistry. 1993;32:889-99.
[41] Zhu J, Liao L, Zhu L, Zhang P, Guo K, Kong J, et al. Size-dependent cellular uptake efficiency, mechanism, and cytotoxicity of silica nanoparticles toward HeLa cells. Talanta. 2013;107:408-15.
[42] Jiang W, Kim BY, Rutka JT, Chan WC. Nanoparticle-mediated cellular response is size-dependent. Nat Nanotechnol. 2008;3:145-50.
[43] Kleinsasser NH, Schmid K, Sassen AW, Harreus UA, Staudenmaier R, Folwaczny M, et al. Cytotoxic and genotoxic effects of resin monomers in human salivary gland tissue and lymphocytes as assessed by the single cell microgel electrophoresis (Comet) assay. Biomaterials. 2006;27:1762-7

[44] Kleinsasser NH, Wallner BC, Harreus UA, Kleinjung T, Folwaczny M, Hickel R, et al. Genotoxicity and cytotoxicity of dental materials in human lymphocytes as assessed by the single cell microgel electrophoresis (comet) assay. J Dent. 2004;32:229-34.
[45] Urban RM, Jacobs JJ, Sumner DR, Peters CL, Voss FR, Galante JO. The bone-implant interface of femoral stems with non-circumferential porous coating. J Bone Joint Surg Am. 1996;78:1068-81.
[46] Rejman J, Oberle V, Zuhorn IS, Hoekstra D. Size-dependent internalization of particles via the pathways of clathrin- and caveolae-mediated endocytosis. The Biochemical journal. 2004;377:159-69.
[47] Conner SD, Schmid SL. Regulated portals of entry into the cell. Nature. 2003;422:37-44.
[48] Kawaguchi H, Ogawa T, Shirakawa M, Okamoto H, Akisaka T. Ultrastructural and ultracytochemical characteristics of multinucleated cells after hydroxyapatite implantation into rat periodontal tissue. J Periodontal Res. 1992;27:48-54.
[49] Travlos GS. Histopathology of bone marrow. Toxicol Pathol. 2006;34:566-98.
[50] Piattelli A, Piattelli M, Mangano C, Scarano A. A histologic evaluation of eight cases of failed dental implants: is bone overheating the most probable cause? Biomaterials. 1998;19:683-90.
[51] Anazawa U, Hanaoka H, Morioka H, Morii T, Toyama Y. Ultrastructural cytochemical and ultrastructural morphological differences between human multinucleated giant cells elicited by wear particles from hip prostheses and artificial ligaments at the knee. Ultrastruct Pathol. 2004;28:353-9.
[52] Midander K, Cronholm P, Karlsson HL, Elihn K, Moller L, Leygraf C, et al. Surface characteristics, copper release, and toxicity of nano- and micrometer-sized copper and copper(II) oxide particles: a cross-disciplinary study. Small. 2009;5:389-99.
[53] Rae T. The toxicity of metals used in orthopaedic prostheses. An experimental study using cultured human synovial fibroblasts. Journal of Bone & Joint Surgery, British Volume. 1981;63:435-40.
[54] Saquib Q, Al-Khedhairy AA, Siddiqui MA, Abou-Tarboush FM, Azam A, Musarrat J. Titanium dioxide nanoparticles induced cytotoxicity, oxidative stress and DNA damage in human amnion epithelial (WISH) cells. Toxicol In Vitro. 2012;26:351-61.
[55] He X, Hartlieb E, Rothmund L, Waschke J, Wu X, Van Landuyt KL, et al. Intracellular uptake and toxicity of three different Titanium particles. Dent Mater. 2015;31:734-44.
[56] Desai MP, Labhasetwar V, Walter E, Levy RJ, Amidon GL. The mechanism of uptake of biodegradable microparticles in Caco-2 cells is size dependent. Pharm Res. 1997;14:1568-73.

6 Own contribution of presented work

The individual contribution of the presented work is shown in the sequence of the authors and coauthors in the presented publications (7.1.1 and 7.1.2).

I am the first author for both of the presented publications. In these both publications i coordinated the cooperations with other working groups and performed the design of the study, data collection, analysis and writing.

Both of the publications were published in the peer reviewed journal “dental materials” (with an impact factor of 3.93 in 2015).

7 Original works

7.1 Publications for the cumulative dissertation

7.1.1 Analysis of titanium and other metals in human jawbones with dental implants – A case series study

He X, Reichl FX, Wang Y, Michalke B, Milz S, Yang Y, Stolper P, Lindemaier G, Graw M, Hickel R, Högg C. Dent Mater. 2016; 32:1042-51.

DENTAL MATERIALS 32 (2016) 1042–1051

Available online at www.sciencedirect.com

ScienceDirect

journal homepage: www.intl.elsevierhealth.com/journals/dema

Analysis of titanium and other metals in human jawbones with dental implants – A case series study

Xiuli He[a,b], Franz-Xaver Reichl[a,b], Yan Wang[a,b], Bernhard Michalke[c], Stefan Milz[d], Yang Yang[a,b], Philipp Stolper[e], Gabriele Lindemaier[f], Matthias Graw[f], Reinhard Hickel[b], Christof Högg[a,b,*]

[a] Department of Operative/Restorative Dentistry, Periodontology and Pedodontics, Ludwig-Maximilians-University of Munich, Goethestr. 70, 80336 Munich, Germany
[b] Walther-Straub-Institute of Pharmacology and Toxicology, Ludwig-Maximilians-University of Munich, Nussbaumstr. 26, 80336 Munich, Germany
[c] Research Unit Analytical Biogeochemistry, Helmholtz Zentrum Munich – German Research Center for Environmental Health (GmbH), Ingolstaedter Landstraße 1, 85764 Neuherberg, Germany
[d] Department of Anatomy II – Neuroanatomy, Ludwig-Maximilians-University of Munich, Pettenkoferstr. 11, 80336 Munich, Germany
[e] Fogra Forschungsgesellschaft Druck e.V., Streitfeldstr 1, 81673 Munich, Germany
[f] Institute of Forensic Medicine, Ludwig-Maximilian-University of Munich, Nussbaumstr. 26, 80336 Munich, Germany

ARTICLE INFO

Article history:
Received 27 October 2015
Received in revised form
23 December 2015
Accepted 31 May 2016

Keywords:
Titanium content
Human jawbones
Dental implants
Ti particles

ABSTRACT

Objective. The aim of this study was to measure titanium (Ti) content in human jawbones and to show that Ti was released from dental implants inserted into these jawbones.
Methods. Seven samples from four human subjects with dental implants were analysed as test group and six bone samples of similar topographical regions from six human subjects without implants served as control. The contents of various elements in human jawbones were detected by inductively coupled plasma optical emission spectrometry. The distributions of various isotopes in human mandibular bone were measured with laser ablation-inductively coupled plasma-mass spectrometry (LA-ICP-MS). Histological analyses of undecalcified, Giemsa-Eosin stained mandible sections were performed by light microscopy and particles were identified in human bone marrow by scanning electron microscope-energy dispersive X-ray analysis.
Results. In test group only Ti content was significantly higher compared to control group. The mean contents of Ti were 1940 μg/kg in test group and 634 μg/kg in control group. The highest Ti content detected in human mandibular bone was 37,700 μg/kg-bone weight. In samples 4–7 (human subjects II–IV), increased Ti intensity was also detected by LA-ICP-MS in human mandibular tissues at a distance of 556–1587 μm from implants, and the intensity increased with decreasing distance from implants. Particles with sizes of 0.5–40 μm were found in human jawbone marrow tissues at distances of 60–700 μm from implants in samples 4–7.

* *Corresponding author at*: Department of Operative/Restorative Dentistry, Periodontology and Pedodontics, LMU Munich, Goethestr. 70, 80336 Munich, Germany. Tel.: +49 89 2180 73842; fax: +49 89 2180 73841.
E-mail address: christof.hoegg@lrz.uni-muenchen.de (C. Högg).
http://dx.doi.org/10.1016/j.dental.2016.05.012

Significance. Ti released from dental implants can be detected in human mandibular bone and bone marrow tissues, and the distribution of Ti in human bone was related to the distance to the implant.

1. Introduction

In the last 50 years titanium (Ti) and its alloys have been widely used for dental and medical applications [1,2]. Clinically, pure Ti (Ti >99%) and the alloy Ti-6Al-4V are mainly used for endosseous implants [2]. Ti alloys with other metals (e.g. nickel (Ni), chromium (Cr), iron (Fe), and molybdenum (Mo)) are applied for implant devices such as bone plates or screws [2,3]. Ti is the main component in those implants/implant devices so that a stable TiO_2 layer [4,5] on the surface can provide Ti based implants/implant devices with a high biocompatibility and resistance to corrosion [6–9].

Although Ti based implants have been considered to be biological inert, it has been found that implants in the body can undergo corrosion and release particulate debris over time [10,11]. It has been reported that the metallic debris from Ti based implants might exist in several forms including particles (micrometer to nanometre size), colloidal and ionic forms (e.g. specific/unspecific protein binding) [12,13], organic storage forms (e.g. hemosiderin, as an iron-storage complex), inorganic metal oxides and salts [12]. According to a previous study [14], the degradation of implants in the human body is primarily induced by wear and corrosion: wear is the mechanical/physical form of implant degradation which produces particles; while corrosion refers to the chemical/electrochemical form of degradation that mainly produces soluble metal ions [14]. Ti particles released from implants have been found in the regenerated bone and peri-implant tissues in animals [7,15]. It has been shown that also Ti ions can be released from embedded implants in animals [16,17]. Ti particles/ions are able to enter the circulation of blood and lymph [12,18,19]. Ti particles detached from hip, knee and mandible implants have been detected in organs such as liver, spleen, lung and lymph nodes [5,19]. Increased levels of elementary Ti have also been detected in the blood of patients with poorly functioning implants [12].

Increased concentrations of metals (e.g. Ti, Cr, Co and Al) derived from implants in body fluids might induce acute or chronic toxicological effects [12]. The long-term effects of Ti derived from implants are still not fully understood, but associated hypersensitivity and allergic reactions in patients have been reported [20,21]. In a clinical study, 0.6% of 1500 patients were found to exhibit Ti allergic reactions [20]. Additionally, it has been found that detached metal debris from implants might cause marrow fibrosis, necrosis and granulomatosis [22–24].

The aim of our study was to measure the release of Ti and other metallic elements from dental implants through detailed post-mortem studies of human subjects with dental implants. In the present study, Ti released from implants inserted into human jawbones was identified and quantified, and the spatial distribution of Ti in human jawbones near implants was also investigated.

2. Materials and methods

2.1. Materials

The test group contained 7 samples from four human subjects with dental implants (Table 1). The control group contained 6 bone samples from similar topographical regions from six human subjects without dental implants.

The bodies were individually donated for medical research. Subjects I–III in the test group and all six of the subjects from the control group were obtained during the dissection course of the anatomical institute of the Ludwig-Maximilian-University Munich. Bone implant sample from subject IV was supplied by the institute of forensic medicine of the Ludwig-Maximilian-University Munich. Subjects I–III carried two implants (one on each side of the mandible) replacing the mandibular canine teeth (FDI System: 33, 43). Subject IV carried two implants that replaced the left first and second molars in the mandible (FDI System: 36 and 37). All the lower jawbones in the test group contained no additional natural teeth. Four out of the six control subjects were toothless as well. The other two control subjects were partially edentulous. The average age of the subjects in the test group (excluding subject IV) and control group were 88 and 85 years, respectively.

For subjects I–III, each of the two implants with the adjacent jawbone was taken as a single sample; for subjects IV, two implants with adjacent jawbone on each side were taken as a single sample. Therefore, there were seven implant samples in our experiment (Table 1). Implants used in samples 5–6 were produced by Astra Tech implant system (Mannheim, Germany), and the implants used for sample 4 and sample 7 were produced by Straumann AG (Basel, Switzerland). The manufacturers of the implants of samples 1–3 were unknown. Due to ethical consideration, it is not possible to get more information about the implants, such as the "age" of the implants (for how many years it has been loaded), the type of the implants and the surface treatment on the implants. Ti dental implants have no identification number to provide detail information (e.g. for age determination).

2.2. Sample analysis by inductively coupled plasma optical emission spectrometry (ICP-OES)

2.2.1. Sample preparation

All 7 samples of test group and all 6 samples of control group had been fixed in 4% buffered formalin (Merck, Darmstadt, Germany). The soft tissue was cautiously removed

Table 1 – Summary information for the test group.

Subject number	Age	Gender	Implants	Sample number	
No. I	98	Female	2 pieces, on the positions of both of the both mandibular canine teeth (FDI System: 33, 43)	No. 1: right mandible segment	No. 2: left mandible segment
No. II	83	Female	2 pieces, on the positions of both of the mandibular canine teeth (FDI System: 33, 43)	No. 3: left mandible segment	No. 4: right mandible segment
No. III	84	Male	2 pieces, on the positions of both of the mandibular canine teeth (FDI System: 33, 43)	No. 5: right mandible segment	No. 6: left mandible segment
No. IV	Unknown	Female	2 pieces, on the positions of the left first and second molars in the lower jaw (FDI System: 36 and 37)	No. 7: left Mandible segment	

with Feather® disposable stainless steel scalpels and then immersed in 100% methanol (Carl Roth, Karlsruhe, Germany).

2.2.1.1. *Test group*. Jawbone slices in the sagittal plane were prepared from samples 1–7 by cutting with a diamond band saw (cut-grinder macro, patho-service GmbH, Oststeinbek, Germany). The samples were cut at intervals of 1 mm in a direction moving toward the implants, and cutting was stopped immediately adjacent to the implant (Fig. 1). From each sample, at least 5 jawbone slices with an approximate thickness of 500 μm were obtained. For analysis the 5 jawbone slices closest to the implant were used.

Each jawbone slice was further divided into 4 quadrants (A–D) (Fig. 1). Each quadrant was weighed and dissolved in 1 ml sub-boiled distilled nitric acid at 170 °C for 12 h. The solution was subsequently diluted (1:5) in Milli-Q Water. The contents of the elements Ti, Al, Cd, Cr, Co, Cu, Fe, Mn, Mo, Ni and V in each quadrant were analysed by ICP-OES (Optima 7300 DV, Perkin Elmer, Rodgau-Jügesheim, Germany). The remaining specimens containing the implant and adjacent bone were reserved for further analysis (Sections 2.3 and 2.4).

2.2.1.2. *Control group*. Control samples were taken from mandibular regions topographically comparable to those bearing the implants. Again 5 adjacent jawbone slices were cut and each of the slices was divided into 4 quadrants. For analysis by ICP-OES, same procedure as samples 1–7 was performed.

2.2.2. *Analytical procedure*

An ICP-OES, Optima 7300 DV system (Perkin Elmer, Rodgau-Jügesheim,Germany) was used for element determination. Sample introduction was carried out using a peristaltic pump connected to a Seaspray nebulizer with a cyclon spray chamber. The measured spectral element lines were (in nm): Al: 167.078, Cd: 214.438, Cr: 267.716, Co: 228.616, Cu: 324.754, Fe: 259.941, Mn: 257.611, Mo: 202.030, Ni: 231.604, V: 292.464, Ti: 334.941.

The RF power was set to 1400 W; the plasma gas was 13 L Ar/min, whereas the nebulizer gas was approximately 0.6 L Ar/min after daily optimization.

Routinely each ten measurements, three blank determinations and a control determination of a certified standard for all mentioned elements were performed. Calculation of results was carried out on a computerized lab-data management system, relating the sample measurements to calibration curves, blank determinations, control standards and the weight of the digested sample.

The volumes of sample digests were sufficient for duplicate measurements ($n = 2$).

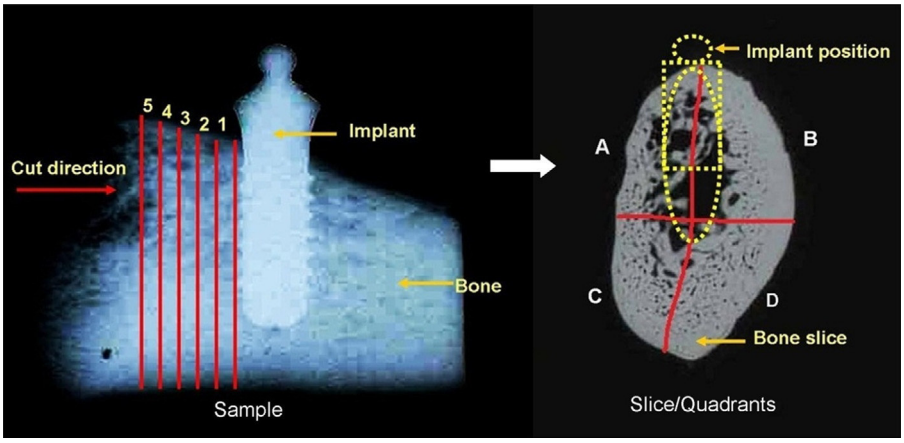

Fig. 1 – Scheme (X-ray image) of the cutting procedure for samples 1–7: at least five bone slices were obtained from each sample; each slice was divided into 4 quadrants (A, B, C and D). The red lines represent the cuts, and the distance between two cuts is 1 mm, the numbers represent slice numbers, number 1 represents the slice closest to implant. (For interpretation of the references to colour in this figure legend, the reader is referred to the web version of this article.)

2.2.3. Calculations and statistics

For a total jaw bone slice the content (μg/kg) of each investigated element was calculated by dividing the summed concentrations of the 4 quadrants with their summed masses.

The results are presented as mean ± standard error of the mean (SEM). Independent two-sample *t*-test and a one-way ANOVA analysis followed by post hoc Bonferroni adjustment were performed for statistical analysis. Differences were considered statistically significant only when the *p*-value was less than 0.05 ($p < 0.05$) [25].

2.3. Content distribution measured by Laser Ablation-Inductively Coupled Plasma-Mass Spectrometry (LA-ICP-MS)

2.3.1. Sample preparation

The remaining parts of samples 4–7 (the bone surrounding the implants) and bone samples from the control group were dehydrated in ascending ethanol fractions (70%, 80%, 90% and 100%), defatted in xylene (Merck, Darmstadt, Germany), and embedded in methylmethacrylate (Fluka, Switzerland). Samples 4–7 were analysed because in these samples significantly higher Ti contents (compared to controls) were detected with ICP-OES measurement in Section 2.2.

Details of the embedding and cutting process can be found in a previous study [26]. The polymerized methacrylate blocks were cut at a thickness of approximately 300 μm parallel to the long axis of the implants in the mesio-distal plane using a Leica SP 1600 saw-microtome (Leica, Wetzlar, Germany). The sections were used for spectroscopy and for histological analysis.

The distribution of the isotopes ^{47}Ti, ^{27}Al, ^{43}Ca, ^{52}Cr, ^{59}Co, ^{63}Cu, ^{57}Fe, ^{39}K, ^{55}Mn, ^{60}Ni, ^{51}V, ^{64}Zn and ^{66}Zn in each section were analysed by Laser Ablation-Inductively Coupled Plasma-Mass Spectrometry (LA-ICP-MS) – NWR-213® (New Wave Research Co. Ltd.) coupled to a NexION® 300 ICP-MS (PerkinElmer).

2.3.2. Analytical procedure

The laser ablations started from the bone region at a distance of 5 mm from the implant and ended in the implant region. In this manner, sample-specific backgrounds could be measured by moving from low to high contents [27], and memory effects were avoided. Two to three parallel ablation lines with each time 6 measurements into the deep (10 μm depth ablation per measurement) were performed for each jawbone slice. The average value of 2–6 measurements was calculated for each line (the first measurement was discarded in order to eliminate possible contamination on the surface of the bone sections which could have occurred during the cutting process). Instrument settings and parameters are shown in Table 2.

After the laser ablations, contact radiographs (Faxitron X-ray Corporation, Lincolnshire, IL, USA) for each section were taken on Agfa Strukturix X-ray sensitive film (Agfa-Gevaert, Mortsel, Belgium). The laser lines were clearly visible on the X-ray film and were photographed with an Axiophot microscope (Zeiss, Goettingen, Germany), equipped with Zeiss Plan-Neofluar objectives (5× and 10×) in transmitted light mode.

Table 2 – Instrument settings for LA-ICP-MS.

Laser	Energy: 0.930 mJ Power: 100% Pulse repetition rate: 10 Hz Scan speed: 35 μm/s Spot size: 50 μm Ablation pattern: line Depth: approx. 10 μm
ICP	Plasma power: 1200 W Transport gas: 1.2 L/min Ar Auxiliary gas: 0.8 L/min Ar Cool gas: 17 L/min Ar
MS	Registered isotopes: ^{47}Ti, ^{27}Al, ^{43}Ca, ^{52}Cr, ^{59}Co, ^{63}Cu, ^{57}Fe, ^{39}K, ^{55}Mn, ^{60}Ni, ^{51}V, ^{64}Zn and ^{66}Zn Dwell time/isotope: 25 ms

2.4. Histological analysis

2.4.1. Sample preparation

From each of the samples 4–7, one of the sections (cutting procedure described in Section 2.3.1) was glued (Cyanolit 201, Panacol LTD., Zürich, Switzerland) on opaque plastic slides, ground thinner, polished (EXAKT® 400CS grinding system, EXAKT Vertriebs GmbH, Norderstedt, Germany) and stained with Giemsa-Eosin stain (Sigma Aldrich, Steinheim, Germany).

The same procedure was applied for the control samples.

2.4.2. Light microscopy observation and scanning electron microscope-energy dispersive X-ray (SEM-EDX) measurements

The stained sections were examined with an Axiophot microscope (Zeiss, Goettingen, Germany) that was equipped with Zeiss Plan-Neofluar objectives (5× and 10×) in transmitted light mode. Images were recorded with an Axciocam HRc digital camera (Zeiss, Goettingen, Germany).

The sections that contained visible dark particles were coated with gold and investigated with a SEM (EVD MA 15) equipped with secondary electron (SE) and back-scattered electron (BSE) detectors. The energy dispersive X-ray (EDX) analyses were performed using an Oxford INCA Penta Fetx 3.

The samples of the control group were also histologically investigated, coated with gold and analysed by SEM-EDX.

3. Results

3.1. Sample analysis by ICP-OES

Among all the investigated elements (Ti, Al, Cd, Cr, Co, Cu, Fe, Mn, Mo, Ni and V), only the element Ti in the test group (samples 1–7) showed significantly higher content compared to the control group ($p < 0.05$).

Ti contents of each total jawbone slice from samples 1–7 and control group are shown in Fig. 2. The highest Ti content (13,205 μg/kg-bone weight) of all slices was detected in sample 6. The average Ti content across all 35 bone slices ($n = 35$) of samples 1–7 (1940 ± 469 μg/kg-bone weight) was significantly higher compared to the average content across the 30 bone slices ($n = 30$) from the control group (634 ± 58 μg/kg-bone weight).

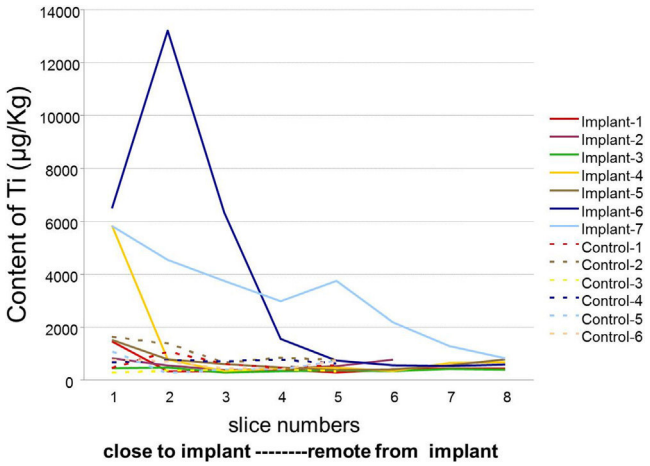

Fig. 2 – Ti contents in the total bone slices from implant samples 1–7 and all control samples. The X-axis represents the number of bone slices; the interval between each two numbers is 1 mm. The Y-axis represents the contents of Ti measured in each total bone slice.

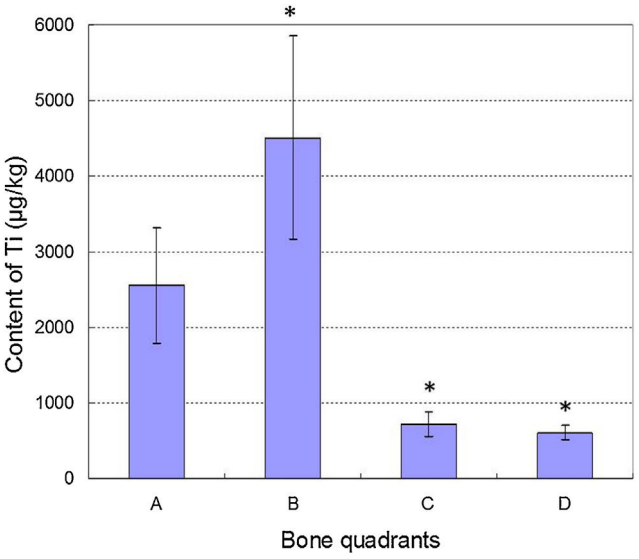

Fig. 4 – The average Ti contents of 4 quadrants of all bone slices from 7 samples in test group (mean ± SEM), $^{*}p < 0.05$.

Ti contents of the total jawbone slices with approximately the same distance from the implant (distance identified by same slice numbers) of all 7 samples are shown in Fig. 3 (mean ± SEM). There were no significant differences in Ti content averages between slices obtained at different distances from the implants ($p > 0.05$).

The average Ti contents for each of the four quadrants (samples 1–7) are shown in Fig. 4. Quadrant B in slice 2 of sample 6 showed the highest Ti content (37,700 µg/kg-bone weight) compared to all the other single quadrants (Fig. 5). The sum of the average Ti contents in the upper half of the bone slice – quadrants A + B (7064 ± 1932 µg/kg-bone weight) – is significantly higher compared to the sum of the average Ti contents in the lower half of bone slice – quadrants C + D (1327 ± 256 µg/kg-bone weight) (Fig. 6). Within the control group there were no significant differences of the Ti contents calculated for all combinations of quadrants or slices.

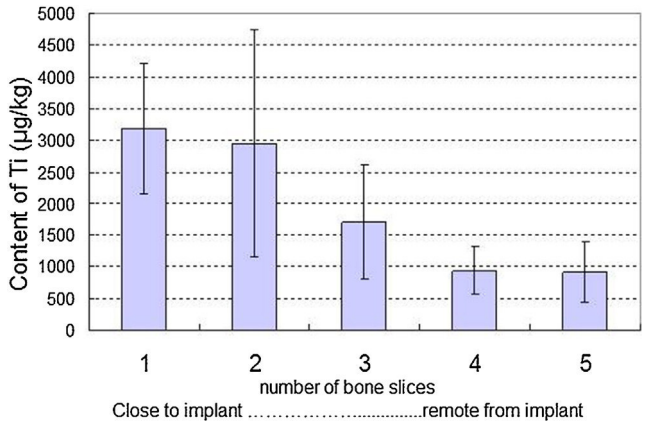

Fig. 3 – Ti contents in each total bone slice in various distances to implants, the x-axis represents the number of bone slices, the interval between each two numbers is 1 mm, and error bars represent the SEMs.

3.2. *Distribution of isotopes measured by LA-ICP-MS*

The isotopes ^{47}Ti, ^{27}Al, ^{43}Ca, ^{52}Cr, ^{59}Co, ^{63}Cu, ^{57}Fe, ^{39}K, ^{55}Mn, ^{60}Ni, ^{51}V, ^{64}Zn and ^{66}Zn in the bone slices with longitudinal cuts through the implants of samples 4–7 (which showed higher Ti content compared to control group measured by ICP-OES) were detected by LA-ICP-MS. Qualitative results are shown in Table 3. ^{47}Ti was the only isotope of all investigated isotopes that could be detected in implant and human jawbone/jawbone marrow tissue of samples 4–7 (with implant) but not in the control samples without implants.

For samples 4–7 along the ablation lines different intensities of ^{47}Ti were detected. In sample 4 the distribution of ^{47}Ti along one ablation line showed that the average ^{47}Ti intensity in a bone region within about 966 µm from the implant is 14 times higher compared to average value of bone at a distance >966 µm from the implant. Samples 5–7 showed comparable

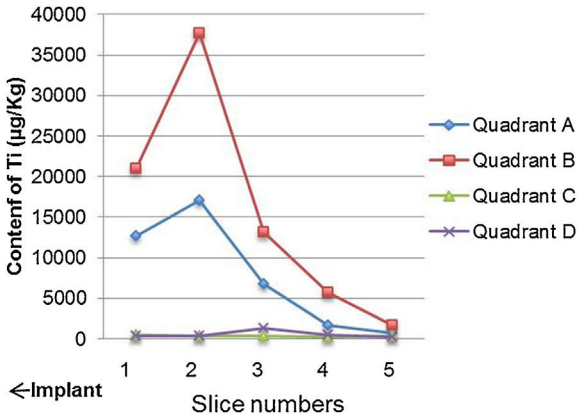

Fig. 5 – Ti contents in 4 quadrants of all slices in sample 6, slice numbers 1–5 represent all slices analyzed in sample 6, number 1 represents the slice closest to implant.

Table 3 – The distribution of the isotopes measured by LA-ICP-MS in the detected bone slices.

Sample numbers	Isotopes in implants (>99%)	Isotopes in bone/bone marrow tissues
4	^{47}Ti (94%), ^{52}Cr (4%), ^{55}Mn (0.55%), ^{56}Fe (0.52%), ^{60}Ni (0.42%)	^{27}Al, ^{39}K, ^{43}Ca, ^{47}Ti, ^{53}Cr, ^{64}Zn, ^{66}Zn
5	^{47}Ti (94.8%), ^{27}Al (4.5%), ^{51}V (0.23%), ^{52}Cr (0.14%)	^{27}Al, ^{39}K, ^{43}Ca, ^{47}Ti, ^{53}Cr, ^{64}Zn, ^{66}Zn
6	^{47}Ti (98.2%), ^{27}Al (0.68%), ^{52}Cr (0.16%)	^{27}Al, ^{39}K, ^{43}Ca, ^{47}Ti, ^{53}Cr, ^{64}Zn, ^{66}Zn
7	^{47}Ti (93.7%), ^{27}Al (5.3%), ^{52}Cr (0.25%), ^{60}Ni (0.21%)	^{27}Al, ^{39}K, ^{43}Ca, ^{47}Ti, ^{64}Zn, ^{66}Zn
Control	–	^{27}Al, ^{39}K, ^{43}Ca, ^{53}Cr, ^{64}Zn, ^{66}Zn

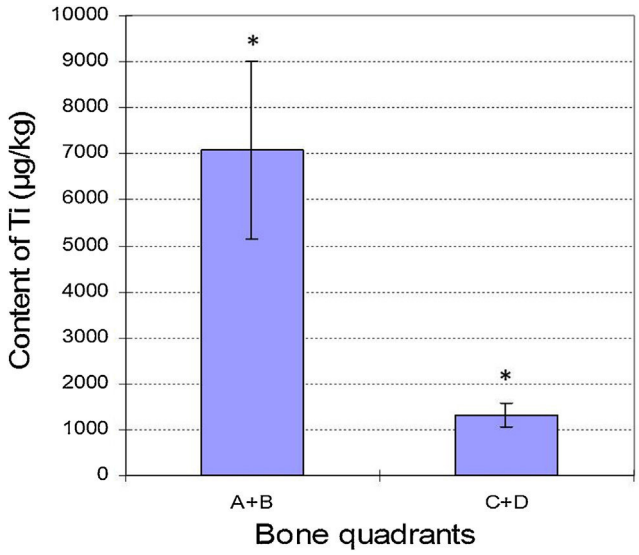

Fig. 6 – The average Ti contents in the upper part (A + B) and lower part (C + D) of each slice in the test group. The error bar represents the SEM, $^{*}p < 0.05$.

results for ^{47}Ti: increased intensities of ^{47}Ti were also detected at distances nearer than 556–1587 μm to the implant surfaces.

Fig. 7 shows the X-ray image of the ablation line in the bone slice of sample 4 combined with LA-ICP-MS results (distributions of ^{43}Ca and ^{47}Ti).

3.3. *Histological analyses*

The histological analysis was performed for samples 4–7 and the control group. Continuous bone contact with the implant

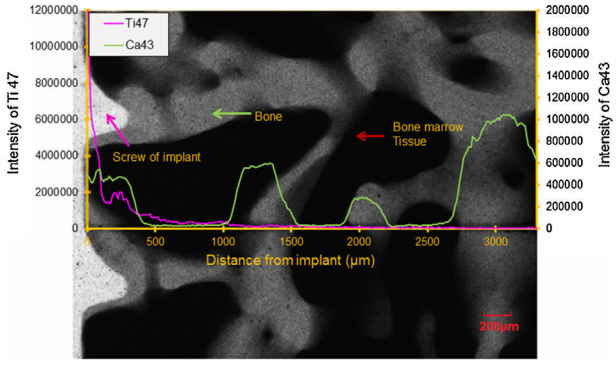

Fig. 7 – X-ray image of one laser ablation line (the part near implant) in sample 4 combined with LA-ICP-MS result (implant screw = white, bone = gray, bone marrow tissues = black).

surface was observed for sample 4 and sample 5 by light microscopy, while observation of samples 6 and 7 showed only bone implant contact at isolated spots. Observation of samples 4–7 by light microscopy revealed black dots between the cells of the bone marrow tissue, which were identified as Ti particles by SEM-EDX analysis. Primary location of Ti particles was in the bone marrow tissue at a distance of 60–700 μm from the implant, with particle sizes <40 μm (Fig. 8a and b). Fig. 8c shows multinucleated cells in the bone marrow tissues near implant. Local avital bone regions were identified in Fig. 8d by the absence of cell nuclei throughout the lacunae of the mineralized tissue. Fig. 8e reveals traces of marrow fibrosis, an indication of previous inflammatory reactions. No Ti particles, no signs of fibrosis, no avital bone tissue and no multinucleated cells were found in the control group (Fig. 8f).

Results of Ti particle identification by SEM-EDX are shown in Fig. 9a–c. Ti particle size measurement revealed sizes from 0.5 to 5 μm (detection limitation of SEM for magnification factor used in present method is 0.5 μm).

4. Discussion

In this study, Ti released from dental Ti implants in human jawbones was measured and identified with ICP-OES, SEM-EDX and LA-ICP-MS. It is very rare to get human jawbones with dental implants. Within 4 years only 7 samples with jaw Ti-implants have been obtained from four human individuals from the anatomical institute and forensic medicine institute of the Ludwig-Maximilians-University Munich. This is the first study investigating Ti release from dental implants in human jawbone.

Due to ethical considerations and privacy protection it is not possible to get more information about the implants, such as the “age” of the implants (for how many years it has been loaded), the type of the implants, the method of surgeon and surface treatment of the implants and impurities present in the implant before insertion. Furthermore, the research in this study is focused on the Ti release from Ti implants in human jawbones compared to controls without Ti implants. Therefore, influences of factors like “age” or “type of implants”, etc. play no role for this research. The individuals in the test and the control groups examined in the present study were highly comparable with respect to age and gender distribution.

4.1. *ICP-OES*

Among the analysed elements Ti, Al, Cd, Cr, Co, Cu, Fe, Mn, Mo, Ni and V, only Ti showed significantly higher contents in the test group compared to the control group.

Ti is commonly used for dental implants [6], and it has already been found that Ti particles can be released into the

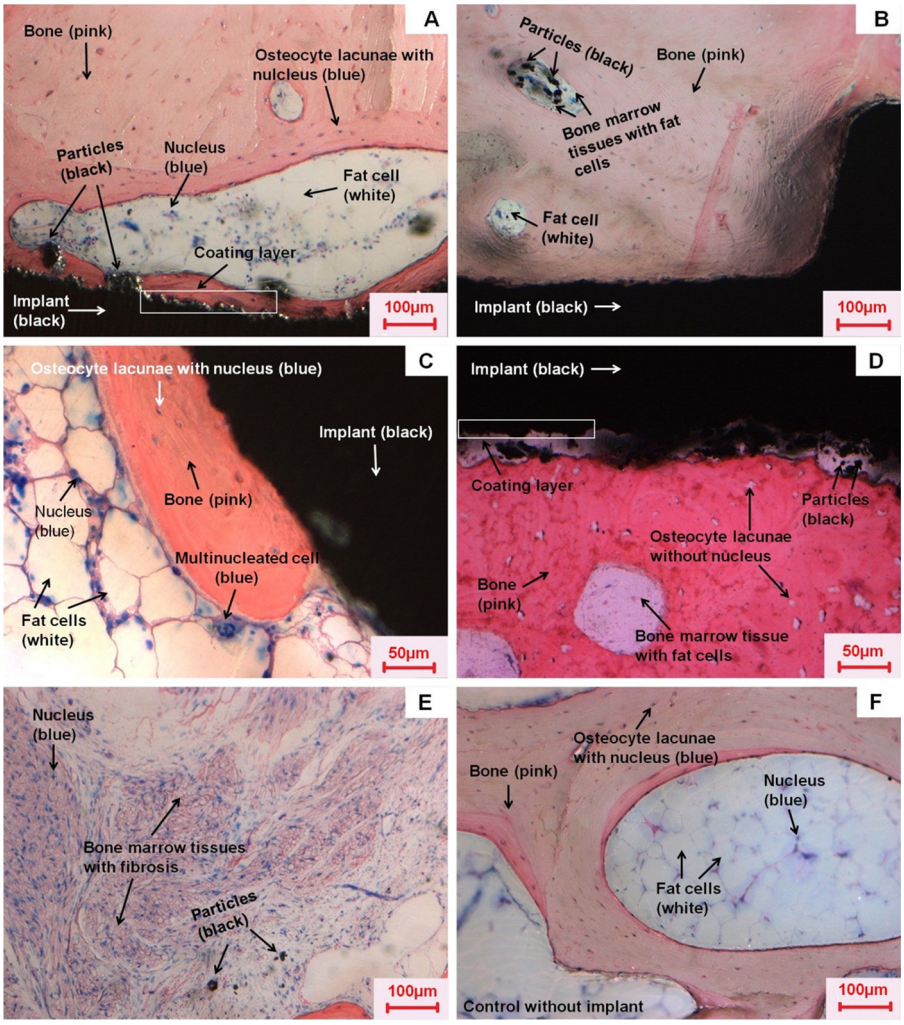

Fig. 8 – The histological images of bone slices with/without implants. Slices (300 μm thick) were glued on opaque plastic slides, ground thinner, polished and stained with Giemsa-Eosin. (a) Bone slice image taken in the combination of transmitted light mode and reflected light mode, a coating layer (marked in rectangle) at the implant surface could be observed with oblique reflected light, particles are visible in bone marrow tissues. The coated implant has a good contact with bone. (b) Particles could be found in bone marrow tissues containing fat cells, and are further identified by SEM-EDX (shown in Fig. 9). The implant has a good contact with bone. (c) Bone slice with multinucleated cell (cell with more than one nucleus) in the bone marrow tissues near the implant. (d) Bone slice with avital bone marrow tissues (identified by the absence of nuclei in the osteocyte lacunae) near the implant. A coating layer (marked with a rectangle) could also be observed. (e) Bone slice with fibrosis in the bone marrow tissues near the implant. (f) Bone slice without implant (control). Fat cell = white, nucleus = blue, particle = black, bone marrow tissues (consist of cells) = white, bone = pink. (For interpretation of the references to colour in this figure legend, the reader is referred to the web version of this article.)

bone tissues from implants [2,14,15]. However, there are less data about the absolute and relative Ti content in human bone surrounding dental implants.

A previous study showed that maximal 4000 μg/kg-bone weight of Ti in rat tibia bone tissues with Ti implant could be detected by ICP-MS after 10 weeks implantation [28]. In the present study, the average content of Ti in the test group measured by ICP-OES (1940 μg/kg-bone weight) was 3 times higher compared to the control group. The highest Ti content of all bone quadrants was 37,700 μg/kg-bone weight. According to previous studies [29,30], Ti particles (<150 μm) exhibited no cytotoxicity in human fibroblasts [29,30], but 10 μg/ml of TiO_2 Nanoparticles (NPs) with a size of 30 nm induced 40% reductions in the cell viabilities of human amnion epithelial cells [30]. Additionally, previous study of our group showed that the EC_{50} of Ti microparticles (<44 μm) in PDL-hTERT cells was above 999 mg/ml, while the EC_{50} of Ti nanoparticles (NPs) (20–250 nm) was 2.84 mg/ml [31]. Regarding the highest Ti content (37,700 μg/kg), the following calculation for rough risk assessment can be given: assuming that Ti in 1 kg bone corresponds to Ti in 1 L fluid, a maximal Ti concentration of 38 μg/ml can be calculated. This value is 3.8 times higher compared to

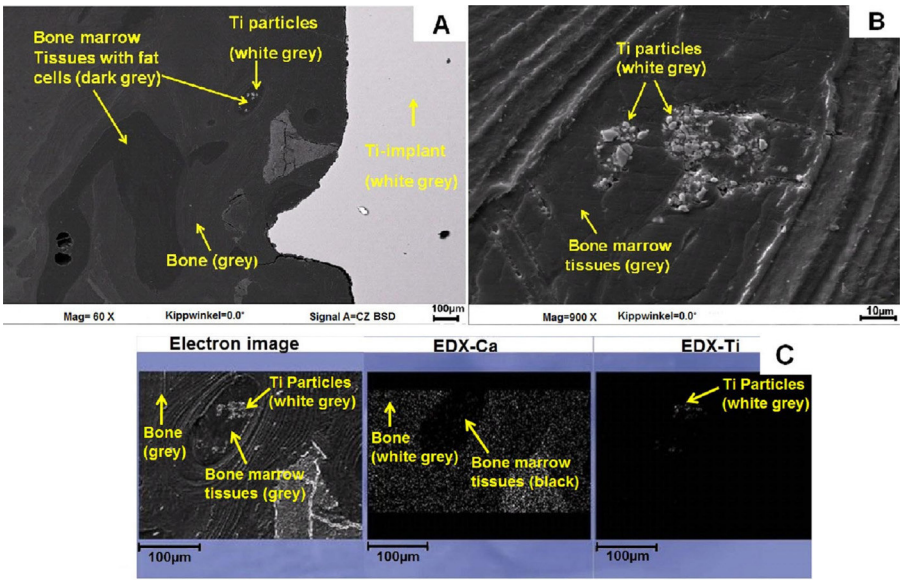

Fig. 9 – SEM image and EDX analysis of the section with particles in Fig. 8(b). (a) Backscattered (BSD) SEM image: Ti implant = white gray, particles = white gray, bone marrow tissues = dark gray, bone = gray. (b) Magnification of the region with particles shown in (a) by SEM. Particles (white gray) could be visualized inside the bone marrow tissues (gray). (c) EDX analysis of the region with particles in (a). On the left is the SEM image of the detected region, in the middle is the intensity of Ca in detected region (bone = gray, bone marrow tissue = black), and on the right is the intensity of Ti in detected region (Ti particles = white gray). The particles in the bone marrow tissues in Fig. 8(b) are identified as Ti particles.

reported cytotoxic concentration (10 μg/ml) of TiO_2 NPs [30] and 74 times lower compared to the EC_{50} (2.84 mg/ml) of Ti NPs [31].

ICP-OES results revealed no distance-dependence of the ^{47}Ti distributions in the total jawbone slices (slice 1–5) of each sample, but the ^{47}Ti contents in the upper quadrants A + B of the bone slices in test group were 5-time higher compared to the lower quadrants C + D. The bone quadrants A + B are anatomically regarded as the alveolar bone, which is known to have a remodeling behavior reacting very sensitive to the transmitted load. Previous studies also reported that the maximum stress (e.g. masticatory forces) is distributed around the implant neck which is surrounded by alveolar bone [32,33]. Obviously, this might explain the higher ^{47}Ti content in the upper quadrants in the current study. Moreover, the main part of the implant is anchored in the upper part of the jawbone, so the upper quadrants A + B of the bone slices are closer to the implant compared to the lower quadrants C + D, and this shorter distance to implant may result in the higher ^{47}Ti content as well. Additionally, the upper quadrants might receive a considerable particle load during the insertion of the implant, which could also lead to higher ^{47}Ti content in the upper quadrants.

4.2. LA-ICP-MS

Due to its flexible spatial analysis capability and high sensitivity, LA-ICP-MS is applied to measure elements, such as Ca, Mg and Sr in bones [27,34]. Moreover, this technique is able to detect unique elemental distributions in micro-spatial areas of dental tissues [35]. In the present study, LA-ICP-MS was used to analyse the region immediately adjacent to the implant because bone slice samples in this region cannot be obtained by the cutting method used for ICP-OES.

The distributions of 13 isotopes ^{47}Ti, ^{27}Al, ^{43}Ca, ^{52}Cr, ^{59}Co, ^{63}Cu, ^{57}Fe, ^{39}K, ^{55}Mn, ^{60}Ni, ^{51}V, ^{64}Zn and ^{66}Zn in bone samples 4–7 with implants were measured by LA-ICP-MS. In bone samples without implant no increased ^{47}Ti was detected. Increased intensity of ^{47}Ti for samples 4–7 was detected in the bone region adjacent to the implant (about 556–1587 μm away from the implant surface). In a previous study, Ti particles from the implant were found in the peri-implant sheep tissue at a distance >200 μm from the implant [15]. Obviously, Ti can migrate from the implant into the surrounding human jawbone or jawbone marrow tissues. In addition, the intensity of ^{47}Ti increased with decreasing distance from the implants, which suggests that the distribution of ^{47}Ti in the jawbone depends on the distance from the implant. This finding is consistent with the ICP-OES results showing that Ti content in upper quadrants A + B (closer to the implant) is significantly higher compared to the lower quadrants C + D. The lack of observations of distance-dependence across the total bone slices by ICP-OES might be attributable to the cutting method not being able to obtain jawbone slices that were sufficiently close to the implant.

^{43}Ca can be taken as an indicator of bone [27]. In this study, ^{43}Ca distribution along the ablation line in the bone slices is shown. Interestingly, ^{47}Ti is present not only in the peri-implant human jawbone marrow tissues but also in the cortical or trabecular bone matrix adjacent to the implant. This is in agreement with previously reported results showing

that Ti particles are found not only in peri-implant animal tissues but also in the bone close to the implants [7,15].

4.3. *Histological analyses*

In the present study, the light microscopy and SEM-EDX results show that Ti particles (0.5–40 μm) are present in human jawbone marrow tissues at a distance of 60–700 μm from the implant. Nearly identical results have been shown by the following studies: Ti particles (from the implant surface) were able to be found in the peri-implant sheep tissue at a distance >200 μm from the implant [15]; Ti particles could not only be observed in peri-implant tissues but also in newly formed bone [7,15]. It was suggested that those Ti particles might be detached during the insertion of the implant [7,36] or released after insertion [14].

In the current study, SEM results showed Ti particles with a size of 0.5–5 μm in human jawbone marrow tissues. Previous studies reported that particles <1 μm could be taken up by non-phagocytic eukaryotic cells via endocytosis [37] and particles with diameters exceeding 0.75 μm can be taken up by macrophages, neutrophils and monocytes via phagocytosis or through macropinocytosis (>1 μm) by all cell types [38]. Therefore, transportation of Ti particles with size of 0.5–5 μm that were observed in human bone marrow tissues of present study into cells is possible. It should also be pointed out that a particle smaller than approximately 1 μm can no longer be seen by transmitted light microscopy.

In this study, bone marrow fibrosis, avital bone tissues and multinucleated cells were observed near the implant. Similarly, a previous post-mortem study about metal particles released from implants showed bone marrow fibrosis in lymph-node tissue [22]. Furthermore, multinucleated cells have been observed after hydroxyapatite implantation in rat periodontal tissues [39]. Bone marrow fibrosis might be induced by marrow injury and inflammation [40]. These effects are reported to be associated with surgical trauma during insertion of implants [41]. Multinucleated giant cells can be elicited by wear particles in periprosthetic tissues in human specimens and these cells might contain phagocytized wear particles [42]. These findings cited above are in accordance with the histological observations made in undecalcified, resin embedded human bone and implant sections in the present study.

5. Conclusion

Ti can be released into human jawbone and jawbone marrow tissues from dental implants. Compared to all other investigated isotopes only ^{47}Ti was observed in both the implants and human bone/bone marrow tissues near the implant but not in the control samples. The intensity of ^{47}Ti in human jawbone increased with decreasing distance to implant. Ti particles in size between 0.5 μm and 40 μm were observed in the jawbone marrow tissues near the implant, which might induce fibrosis and multinucleated cells. Based on our study with a small sample size we suggest that Ti dental implants might have no adverse clinical effects.

Acknowledgements

This study was financially supported by the China Scholarship Council (CSC, 201206220099). We would like to thank Mr. Peter Grill and Mr. Stefan Schulz for the technical support.

REFERENCES

[1] Lautenschlager EP, Monaghan P. Titanium and titanium alloys as dental materials. Int Dent J 1993;43:245–53.
[2] Elias C, Lima J, Valiev R, Meyers M. Biomedical applications of titanium and its alloys. JOM 2008;60:46–9.
[3] McCracken M. Dental implant materials: commercially pure titanium and titanium alloys. J Prosthodont 1999;8:40–3.
[4] Kasemo B. Biocompatibility of titanium implants: surface science aspects. J Prosthet Dent 1983;49:832–7.
[5] Schliephake H, Reiss G, Urban R, Neukam FW, Guckel S. Metal release from titanium fixtures during placement in the mandible: an experimental study. Int J Oral Maxillofac Implants 1993;8:502–11.
[6] Okabe T, Hero H. The use of titanium in dentistry. Cells Mater (USA) 1995;5:211–30.
[7] Franchi M, Bacchelli B, Martini D, Pasquale VD, Orsini E, Ottani V, et al. Early detachment of titanium particles from various different surfaces of endosseous dental implants. Biomaterials 2004;25:2239–46.
[8] Adya N, Alam M, Ravindranath T, Mubeen A, Saluja B. Corrosion in titanium dental implants: literature review. J Indian Prosthodont Soc 2005;5:127.
[9] Velasco-Ortega E, Jos A, Cameán AM, Pato-Mourelo J, Segura-Egea JJ. *In vitro* evaluation of cytotoxicity and genotoxicity of a commercial titanium alloy for dental implantology. Mutat Res/Genet Toxicol Environ Mutagen 2010;702:17–23.
[10] Meachim G, Williams D. Changes in nonosseous tissue adjacent to titanium implants. J Biomed Mater Res 1973;7:555–72.
[11] Galante JO, Lemons J, Spector M, Wilson Jr PD, Wright TM. The biologic effects of implant materials. J Orthop Res 1991;9:760–75.
[12] Hallab NJ, Mikecz K, Vermes C, Skipor A, Jacobs JJ. Orthopaedic implant related metal toxicity in terms of human lymphocyte reactivity to metal-protein complexes produced from cobalt-base and titanium-base implant alloy degradation. Mol Cell Biochem 2001;222:127–36.
[13] Hallab NJ, Jacobs JJ, Skipor A, Black J, Mikecz K, Galante JO. Systemic metal-protein binding associated with total joint replacement arthroplasty. J Biomed Mater Res 2000;49:353–61.
[14] Jacobs JJ, Gilbert JL, Urban RM. Current concepts review – corrosion of metal orthopaedic implants. J Bone Jt Surg 1998;80:268–82.
[15] Martini D, Fini M, Franchi M, Pasquale VD, Bacchelli B, Gamberini M, et al. Detachment of titanium and fluorohydroxyapatite particles in unloaded endosseous implants. Biomaterials 2003;24:1309–16.
[16] Edwin SH. Characteristics of trace ions released from embedded metal implants in the rabbit; 1962.
[17] Ducheyne P, Willems G, Martens M, Helsen J. In vivo metal-ion release from porous titanium-fiber material. J Biomed Mater Res 1984;18:293–308.
[18] Brien WW, Salvati EA, Betts F, Bullough P, Wright T, Rimnac C, et al. Metal levels in cemented total hip arthroplasty. A comparison of well-fixed and loose implants. Clin Orthop Relat Res 1992:66–74.

[19] Urban RM, Jacobs JJ, Tomlinson MJ, Gavrilovic J, Black J, Peoc'h M. Dissemination of wear particles to the liver, spleen, and abdominal lymph nodes of patients with hip or knee replacement. J Bone Jt Surg Am 2000;82:457–76.
[20] Sicilia A, Cuesta S, Coma G, Arregui I, Guisasola C, Ruiz E, et al. Titanium allergy in dental implant patients: a clinical study on 1500 consecutive patients. Clin Oral Implants Res 2008;19:823–35.
[21] Lalor PA, Revell PA, Gray AB, Wright S, Railton GT, Freeman MA. Sensitivity to titanium. A cause of implant failure? J Bone Jt Surg Br 1991;73:25–8.
[22] Case CP, Langkamer VG, James C, Palmer MR, Kemp AJ, Heap PF, et al. Widespread dissemination of metal debris from implants. J Bone Jt Surg Br 1994;76:701–12.
[23] Amstutz HC, Campbell P, Kossovsky N, Clarke IC. Mechanism and clinical significance of wear debris-induced osteolysis. Clin Orthop Relat Res 1992:7–18.
[24] Dannenmaier WC, Haynes DW, Nelson CL. Granulomatous reaction and cystic bony destruction associated with high wear rate in a total knee prosthesis. Clin Orthop Relat Res 1985;22:4–30.
[25] Kim JH, Jung Y, Kim BS, Kim SH. Stem cell recruitment and angiogenesis of neuropeptide substance P coupled with self-assembling peptide nanofiber in a mouse hind limb ischemia model. Biomaterials 2013;34:1657–68.
[26] Milz S, Putz R. Quantitative morphology of the subchondral plate of the tibial plateau. J Anat 1994;185:103–10.
[27] Gruhl S, Witte F, Vogt J, Vogt C. Determination of concentration gradients in bone tissue generated by a biologically degradable magnesium implant. J Anal Atomic Spectrom 2009;24:181–8.
[28] Niinomi M. Metals for biomedical devices. Elsevier; 2010.
[29] Rae T. The toxicity of metals used in orthopaedic prostheses. An experimental study using cultured human synovial fibroblasts. J Bone Jt Surg Br Vol 1981;63:435–40.
[30] Saquib Q, Al-Khedhairy AA, Siddiqui MA, Abou-Tarboush FM, Azam A, Musarrat J. Titanium dioxide nanoparticles induced cytotoxicity, oxidative stress and DNA damage in human amnion epithelial (WISH) cells. Toxicol In Vitro 2012;26:351–61.
[31] He X, Hartlieb E, Rothmund L, Waschke J, Wu X, Van Landuyt KL, et al. Intracellular uptake and toxicity of three different titanium particles. Dent Mater 2015;31:734–44.
[32] Himmlova L, Dostalova T, Kacovsky A, Konvickova S. Influence of implant length and diameter on stress distribution: a finite element analysis. J Prosthet Dent 2004;91:20–5.
[33] Baggi L, Cappelloni I, Di Girolamo M, Maceri F, Vairo G. The influence of implant diameter and length on stress distribution of osseointegrated implants related to crestal bone geometry: a three-dimensional finite element analysis. J Prosthet Dent 2008;100:422–31.
[34] Prohaska T, Latkoczy C, Schultheis G, Teschler-Nicola M, Stingeder G. Investigation of Sr isotope ratios in prehistoric human bones and teeth using laser ablation ICP-MS and ICP-MS after Rb/Sr separation. J Anal Atomic Spectrom 2002;17:887–91.
[35] Kang D, Amarasiriwardena D, Goodman AH. Application of laser ablation-inductively coupled plasma-mass spectrometry (LA-ICP-MS) to investigate trace metal spatial distributions in human tooth enamel and dentine growth layers and pulp. Anal Bioanal Chem 2004;378: 1608–15.
[36] Flatebo RS, Hol PJ, Leknes KN, Kosler J, Lie SA, Gjerdet NR. Mapping of titanium particles in peri-implant oral mucosa by laser ablation inductively coupled plasma mass spectrometry and high-resolution optical darkfield microscopy. J Oral Pathol Med 2011;40:412–20.
[37] Rejman J, Oberle V, Zuhorn IS, Hoekstra D. Size-dependent internalization of particles via the pathways of clathrin- and caveolae-mediated endocytosis. Biochem J 2004;377:159–69.
[38] Conner SD, Schmid SL. Regulated portals of entry into the cell. Nature 2003;422:37–44.
[39] Kawaguchi H, Ogawa T, Shirakawa M, Okamoto H, Akisaka T. Ultrastructural and ultracytochemical characteristics of multinucleated cells after hydroxyapatite implantation into rat periodontal tissue. J Periodontal Res 1992;27:48–54.
[40] Travlos GS. Histopathology of bone marrow. Toxicol Pathol 2006;34:566–98.
[41] Piattelli A, Piattelli M, Mangano C, Scarano A. A histologic evaluation of eight cases of failed dental implants: is bone overheating the most probable cause. Biomaterials 1998;19:683–90.
[42] Anazawa U, Hanaoka H, Morioka H, Morii T, Toyama Y. Ultrastructural cytochemical and ultrastructural morphological differences between human multinucleated giant cells elicited by wear particles from hip prostheses and artificial ligaments at the knee. Ultrastruct Pathol 2004;28:353–9.

7.1.2 Intracellular uptake and toxicity of three different Ti particles

He X, Hartlieb E, Rothmund L, Waschke J, Wu X, Van Landuyt KL, Milz S, Michalke B, Hickel R, Reichl FX, Högg C. Dent Mater. 2015; 31(6):734-44

DENTAL MATERIALS 31 (2015) 734–744

Available online at www.sciencedirect.com

ScienceDirect

journal homepage: www.intl.elsevierhealth.com/journals/dema

Intracellular uptake and toxicity of three different Titanium particles

Xiuli He[a,b], *Eva Hartlieb*[c], *Lena Rothmund*[a,b], *Jens Waschke*[c], *Xiao Wu*[d], *Kirsten L. Van Landuyt*[e], *Stefan Milz*[f], *Bernhard Michalke*[g], *Reinhard Hickel*[b], *Franz-Xaver Reichl*[a,b], *Christof Högg*[a,b,*]

[a] *Department of Operative/Restorative Dentistry, Periodontology and Pedodontics, Ludwig-Maximilians-University of Munich, Goethestr 70, 80336 Munich, Germany*

[b] *Walther-Straub-Institute of Pharmacology and Toxicology, Ludwig-Maximilians-University of Munich, Nussbaumstr 26, 80336 Munich, Germany*

[c] *Institute of Anatomy and Cell Biology, Ludwig-Maximilians-University of Munich, Pettenkoferstr 11, 80336 Munich, Germany*

[d] *Helmholtz Zentrum München-German Research Center for Environmental Health, Cooperation Group of Comprehensive Molecular Analytics, Ingolstädter Landstr 1, 85764 Neuherberg, Germany*

[e] *KU Leuven BIOMAT, Department of Oral Health Sciences, KU Leuven, Kapucijnenvoer 7, 3000 Leuven, Belgium*

[f] *Department of Anatomy II – Neuroanatomy, Ludwig-Maximilians-University of Munich, Pettenkoferstr 11, 80336 Munich, Germany*

[g] *Research Unit Analytical Biogeochemistry, Helmholtz Zentrum Munich-German Research Center for Environmental Health (GmbH), Ingolstädter Landstr 1, 85764 Neuherberg, Germany*

ARTICLE INFO

Article history:
Received 9 December 2014
Received in revised form
17 February 2015
Accepted 31 March 2015

Keywords:
Titanium
Nanoparticles
Cytotoxicity
Cellular uptake
DNA damage

ABSTRACT

Introduction. Titanium (Ti) and its alloys are used for implants and other dental materials. In this study, cytotoxicity, DNA damage, cellular uptake and size of three kinds of Ti particles were measured.

Methods. Cytotoxicity for Ti microparticles (Ti-MPs, <44 μm), NiTi microparticles (NiTi-MPs, <44 μm), and Ti nanoparticles (Ti-NPs, <100 nm) in periodontal ligament (PDL)-hTERT cells was measured with XTT test. DNA damage was determined with comet assay. Particle size was measured with scanning electron microscope, intracellular uptake was determined with laser scanning confocal microscopy and transmission electron microscopy.

Results. The EC_{50} values of investigated particles were: 2.8 mg/ml (Ti-NPs), 41.8 mg/ml (NiTi-MPs) and >999 mg/ml (Ti-MPs). The Olive Tail Moment (OTM) values at 1/10 EC_{50} were: 3.2 (Ti-NPs) and 2.2 (NiTi-MPs). An OTM of 2.2 for Ti-MPs was detected at the concentration of 6666 μg/ml. Determined sizes of investigated particles were 20–250 nm (Ti-NPs), 0.7–90 μm (NiTi-MPs) and 0.3–43 μm (Ti-MPs). The highest cellular uptake efficiency was observed with Ti-NPs, followed by Ti-MPs and NiTi-MPs. Only Ti-NPs were found in the nucleus.

* *Corresponding author at*: Department of Operative/Restorative Dentistry, Periodontology and Pedodontics, LMU Munich, Goethestr 70, 80336 Munich, Germany. Tel.: +49 89 2180 73842; fax: +49 89 2180 73841.
E-mail address: christof.hoegg@lrz.uni-muenchen.de (C. Högg).

http://dx.doi.org/10.1016/j.dental.2015.03.017

Conclusion. Compared to Ti-MPs and NiTi-MPs, Ti-NPs induced higher cellular uptake efficiency and higher toxic potential in PDL-hTERT cells. Ni in the alloy NiTi induced an increase in the toxic potential compared to Ti-MPs.

1. Introduction

Titanium (Ti) and its alloys have been used as source materials for biomedical applications especially in dentistry, since previous studies showed that these materials stand out for good mechanical properties, excellent corrosion resistance and high biocompatibility [1–4]. For example, it was found that Ti is one of the most biocompatible metallic materials because of its ability to form a stable and insoluble protective oxide layer (TiO_2) on its surface [5,6]. Ti is preferentially used for endosseous dental implant material [6]. Besides Ti, some Titanium alloys are also used for dental applications, such as Nickel Titanium (NiTi). The alloy NiTi is used for castings of crowns and denture construction, orthodontic archwires and brackets [7,8]. Recently it has been found that the properties of Ti implants can be improved by using nanostructured Ti consisting of Ti-nanoparticles (Ti-NPs) [9].

Even though Ti based implants are considered to be biocompatible, their induced side effects such as hypersensitivity and allergic reactions have been reported [10–12]. It has also been found that Ti based materials can cause immunoinflammatory reactions [13]. These side effects might have been caused by the interaction between tissues and implants [14,15]. Previous in vitro and in vivo studies showed that Ti ions can be released from Ti based implants, for example by corrosion, wear and electrochemical processes [16–20]. The release of Ni ions from NiTi alloy also has been reported [8]. Previous studies indicated that Ti ions and Ni ions induced cytotoxicity/DNA damage in human cells [21,22]. Furthermore, Ti-particles/debris (3–250 μm) was found in the peri-implant animal tissues after application of Ti based implants [23,24]. Clinical studies also showed that Ti particles in nanometer- and micrometer-size could be released into human tissues/organs of the patients with Ti based implants or replacements [21,25,26]. The toxic effect of Ti-particles has been described in the literature: phagocytosis of Ti-particles could induce cytotoxicity in rat calvarial osteoblasts and MG63 cells [27,28]; Genotoxic effect of Ti-particles has also been detected, which induced apoptosis in mesenchym stem cells [29,30].

It was found that the particles size can influence the toxicity of metal particles [31,32]. The ability of different particles entering cells may also affect the toxicity [31–33], and it is reported that particle size can impact the cellular uptake efficiency and pathway [34–36]. There is less data about toxicity and cellular uptake for Ti-NPs and Ti-MPs available.

The aim of this study is to compare the toxicity and cellular uptake of nanometer-sized Ti, micrometer-sized Ti and NiTi particles, which can be released from dental implants or replacements. In this study, Ti-NPs (Ti 98.5%, <100 nm), Ti-microparticles (Ti-MPs) (Ti 99%, <44 μm) and NiTi-microparticles (NiTi-MPs) (Ni 30%, Ti 70% and <44 μm) were investigated. The cytotoxicity, genotoxicity, and cellular uptake efficiency of these investigated particles have been measured in periodontal ligament (PDL) cells.

2. Materials and methods

2.1. Cell culture

Clinically, PDL cells are the cells growing around natural teeth, which work as the tooth anchor and sustain bone regeneration [37]. PDL cells can provide the implants with the same mobility as natural teeth and reduce the bone loss around implants [38]. Therefore, dental implants combined with PDL would represent a great new therapeutic tool to replace lost teeth [37,38]. Studies have demonstrated the PDL formation on the surface of Ti implants [37,39].

Periodontal ligament with lentiviral gene transfer of human telomerase reverse transcriptase cells (PDL-hTERT cells) were obtained from Experimental Surgery and Regenerative Medicine, Department of Surgery, Ludwig-Maximilians-University (LMU), Munich, Germany [40]. The reason why PDL-hTERT cells were used is that PDL-hTERT cells have extended lifespan with identical morphology compared to the primary PDL cells [40]. The extended lifespan is of great importance to the PDL engineering. PDL-hTERT cells were cultured in a 250 ml tissue culture flask (BD falcon, Franklin Lakes, USA) at 37 °C and 100% humidity with 5% CO_2. The VLE (very low endotoxin) Dulbecco's Minimum Essential Medium (MEM) with 4.5 g/l D-Glucose (Biochrom, Berlin, Germany) was supplemented with 1% penicillin/streptomycin (Biochrom, Berlin, Germany) and 10% Fetal Bovine Serum (Sigma–Aldrich, Munich, Germany).

2.2. Particle exposure and size measurement

Ti-MPs (99%; <44 μm (−325 mesh)) and NiTi-MPs (70% Ti, 30% Ni; <44 μm (−325 mesh)) were obtained from Alfa Aesar, Karlsruhe, Germany. Ti-NPs contained 98.5% Ti < 100 nm (Sigma–Aldrich, St. Louis, USA). Fresh suspensions of Ti-MPs, NiTi-MPs and Ti-NPs were prepared for each experiment. The stock solutions were prepared by adding investigated particles (1000 mg Ti-MPs, 150 mg NiTi-MPs, and 21.8 mg Ti-NPs) into 3 ml of medium and well mixed. To determine the exact concentrations of particles, 200 μl of stock solution was evaporated at 70 °C to complete dryness and the average net weight of the particles was measured six times. The final exposure concentrations (particle weight/0.1 ml) were obtained by adding different volumes of stock solution. The exposure concentrations of the investigated particles for each test are shown in Table 1.

Table 1 – Concentrations of Ti-MPs, NiTi-MPs and Ti-NPs used in XTT viability assay, trypan blue test and comet assay.

XTT viability assay (μg/ml)			Trypan blue test (μg/ml)			Comet assay (μg/ml)		
Ti-MPs	NiTi-MPs	Ti-NPs	Ti-MPs	NiTi-MPs	Ti-NPs	Ti-MPs	NiTi-MPs	Ti-NPs
999,000	83,400	13,080	33,300	20,900	1420	6666	4180	284
300,000	55,600	4360	6660	4180	284	3333	836	57
103,000	16,680	1308	3330	836	56	666	418	28
33,000	5560	436	666	418	28	333	209	14
	1670	131						

The size of investigated particles was determined with Scanning Electron Microscopy (SEM) LEO 1550 (Zeiss, Oberkochen, Germany) by measuring the minimal Feret distance [41]. 4× 200 single particles of each investigated particle sample were used for particle size measurement. In case of spontaneous combustion Ti-NPs were suspended in PBS (phosphate buffered saline) before measurement.

2.3. XTT viability assay

XTT-based cell viability assay was applied to determine the half-maximum effect concentration (EC_{50}) values for the investigated particles in PDL-hTERT cells. In this assay, a concentration of 20,000 cells/well (in 0.1 ml medium) was incubated for 24 h in the 96-well plate (BD falcon, Heidelberg, Germany). Then the cells were treated with different concentrations (Table 1) of Ti-NPs, Ti-MPs and NiTi-MPs. Negative control cells received medium only. Positive control cells received 1% Triton X-100. After exposure of cells to investigated particles for 24 h, 50 μl XTT (1 mg/ml) solution (sodium 30-[1-(phenyl-aminocarbonyl)-3,4-tetrazolium]-bis(4-methoxy-6-nitro)benzene sulfonic acid hydrate) labeling agent (in RPMI (Roswell Park Memorial Institute medium) 1640 without phenol red) and electron-coupling reagent PMS (N-methyldibenzopyrazine methylsulfate in PBS) (0.383 mg/ml) were added (cell proliferation kit II; Roche Diagnostics GmbH Penzberg, Germany). After 4 h incubation the photometric analysis was performed in another well plate to determine formazan values.

The formazan values were referred to positive and negative control. EC_{50} values were obtained by fitting the data to a dose–effect sigmoidal curve using GraphPad prism 4 (GraphPad Software, Inc. La Jolla, USA). Each experiment was repeated four times ($n = 4$).

2.4. Cell death detected with trypan blue staining

Trypan blue staining reveals the ratio of live and dead cells. Non-viable cells are stained blue since the cell membrane of non-viable cells is permeable for trypan blue [42]. The cells were treated with different concentrations (Table 1) of investigated particles for 24 h. After the treatment, the cells were washed three times with PBS. To detach cells from the 12-well plate, the cells were treated with trypsin at 37 °C for 5 min. The trypsin effect was stopped by adding medium. Afterwards, the cells were stained with 0.4% trypan blue (Sigma Aldrich, Steinheim, Germany) for 3 min. Ratio of dead cells was counted in neubauer chamber (Paul Marienfeld Lauda-Königshofen, Germany) (100–120 cells). Negative control cells received medium only. Each experiment was repeated three times ($n = 3$).

2.5. Comet assay

DNA damage of investigated particles was analyzed by the alkaline single-cell microgel electrophoresis (comet) assay. This comet assay method has been described in our previous studies [42,43]. Experiment was conducted in red light. Slides (26 mm × 76 mm, R. Langenbrinck, Emmendingen, Germany) were coated with a layer of 85 μl 0.5% agarose (Biozym, Oldendorf, Germany), and then dried for one week at 25 °C excluding daylight.

PDL-hTERT cells (2×10^5) were cultured in 1 ml medium in a 12-well plate (BD falcon, Heidelberg, Germany) for 24 h. Afterwards, the cells were exposed to different concentrations (Table 1) of all investigated particles for further 24 h. Then cells were washed with 1 ml PBS three times, and treated with 100 μl trypsin at 37 °C for 5 min, 300 μl medium was added to stop the effect of trypsin. The cell suspension was then centrifuged (800 rpm, 10 min), and the supernatant was discarded. The cell pellets were re-suspended in 400 μl PBS and centrifuged again. Cell pellets were suspended in 25 μl PBS, and mixed with 75 μl LMP-Agarose (low melting point) (Biozym, Oldendorf, Germany), and then transferred onto the pre-coated slides (as described above). A covering glass (24 mm × 60 mm) (R. Langenbrinck, Emmendingen, Germany) was placed on the top of the slide. The slide was then kept at 4 °C for at least 5 min, and another layer of agarose was over stacked. After incubation at 4 °C for 5 min, the covering glass was removed, and the slide was stored in lysis buffer (2.5 M NaCl, 100 mM EDTA, 10 mM Tris, 1% Na-lauroylsarcosinate, H_2O; pH = 10; before use 1% Triton X-100 and 10% dimethylsulfoxide were added) overnight.

Before electrophoresis, the slides were placed in the alkaline electrophoresis solution (6 °C) for 30 min. Electrophoresis was conducted at 6 °C with 25 V, maximum 300 mA for 30 min. The slides were then washed with 400 mM Tris buffer (Merck, Darmstadt, Germany) and stained with 50 μl 200 μg/ml ethidium bromide (Sigma–Aldrich, St. Louis, USA). The slides were evaluated using an Olympus BX 60 fluorescence microscopy (Olympus, Hamburg, Germany) with a 40× objective and the software program comet assay II (Perceptive Instrument Ltd., Haverhill, UK). Positive control cells received 100 μM methyl methanesulfonate (MMS) (Sigma–Aldrich, Steinheim, Germany) and negative control cells received medium only. For each sample, about 50 cells were investigated. The test was repeated six times ($n = 6$). Olive tail moment (OTM) as a product of the tail length and the percentage of total DNA in the tail was applied to evaluate DNA damage [42,43].

2.6. Cellular uptake

2.6.1. Laser scanning confocal microscopy (LSCM) measurement

Cellular and intracellular uptake of Ti-NPs, Ti-MPs and NiTi-MPs in PDL-hTERT cells was determined with LSM 510 (Zeiss, Oberkochen, Germany), as described in a previous study [44]. It was found that noble metals can be used as marker for cellular imaging of LSCM due to their surface plasmon resonance [45,46]. Similarly, Ti-NPs, Ti-MPs and NiTi-MPs also emit intensive light in a close proximity to the wavelength (633 nm) of the laser. The nucleus was stained with Sybr green I nucleic acid gel stain (Invitrogen, Oregon, USA). For visualization of the cells the plasma membrane was stained with cell mask membrane plasma orange stain (Invitrogen, Oregon, USA). Sybr green I and cell mask membrane plasma orange were excited by 488 nm and 543 nm.

The cells were cultured for 24 h on a covering glass in 24-well plate (BD Falkon, Franklin lakes, USA) and then exposed to Ti-NPs (28 μg/ml (1/100 EC_{50}), 56 μg/ml (1/50 EC_{50})), NiTi-MPs (418 μg/ml (1/100 EC_{50}), 4180 μg/ml (1/10 EC_{50})) and Ti-MPs (418 μg/ml) for another 24 h. After that, the cells were carefully shaken, washed with PBS three times and stained with 2.5 μg/ml of Cell Mask Membrane Plasma Orange at 37 °C for 5 min. The cells were then fixed with 2% paraformaldehyde (Carl Roth, Karlsruhe, Germany), washed three times with PBS, and stained with Sybr green I (1:50,000) at 25 °C for 15 min. The covering glasses were mounted on microscopic slides using prolong gold antifade reagent with 4′,6-diamidin-2-phenylindol (DAPI) (Invitrogen, Oregon, USA) after they were washed three times with PBS. Samples were kept at 4 °C before analysis. With the LSCM, a stack of images at different points along the Z-axis was performed in the direction away from the cover slip and moving into the cells. For each experiment about 60 cells were investigated and the experiment was repeated four times ($n = 4$).

2.6.2. Transmission electron microscopy (TEM) measurement

TEM Libra 120 (Zeiss, Oberkochen, Germany) was used to confirm the cellular uptake of Ti-NPs. Ti-MPs and NiTi-MPs were not investigated due to the technical difficulties obtaining ultra thin sections from large particles. PDL-hTERT cells were treated with Ti-NPs (28 μg/ml) for 24 h. After the incubation with Ti-NPs, the cells were washed with PBS three times and fixed with 2% glutaraldehyde in 0.1 M PBS buffer at 25 °C for at least 2 h. Fixed cells were washed with PBS three times and then treated with 1% osmium tetroxide (Merck, Darmstadt, Germany) at 25 °C for 1 h. The dehydration was performed with ascending concentrations of ethanol: 30%, 50%, 70%, 90% and 100% (ethanol purity ≥ 99.8%, Carl Roth, Karlsruhe, Germany). Afterwards, cells were embedded in epon 812 (Serva, Heidelberg, Germany). After the resin blocks were hardened, they were cut into ultra thin sections (70–90 nm) with an ultra-microtome (Zeiss, Oberkochen, Germany), and then contrasted with 2% uranyl acetate (Merck, Darmstadt, Germany) followed by Pb-citrate (Merck, Darmstadt, Germany). The ultra thin sections were analysed.

To obtain morphology and size, suspensions of Ti-NPs in water were evaporated to dryness on TEM grids and observed with TEM.

2.7. Statistic analysis

The results were presented as mean ± standard deviation (SD). To analyze the effect of particles on cytotoxicity, DNA damage, and cellular uptake, a one-way ANOVA analysis followed by Tukey's test was applied. Differences were considered statistically significant only when the p-value was less than 0.05 ($p < 0.05$) [47].

3. Result

3.1. Particle size measurement

It was found that about 90% of Ti-NPs were sized below 100 nm and 0.6% of Ti-NPs were sized above 200 nm. Ti-MPs were sized between 0.3 μm and 43 μm; more than 50% of the particles were sized below 5 μm. NiTi-MPs were sized between 0.7 μm and 90 μm, 60% of the particles were sized above 10 μm and 17% of small particles were sized below 5 μm. The particle size distributions of all investigated particles are shown in Table 2.

3.2. Cytotoxicity

3.2.1. XTT viability assay

The EC_{50} values for Ti-NPs, Ti-MPs and NiTi-MPs in PDL-hTERT cells were determined and a relative toxicity was calculated (Table 3). Ti-NPs had the highest toxic potential ($EC_{50} = 2.84 \pm 0.37$ mg/ml; mean ± SD, $n = 4$). EC_{50} value of NiTi was 41.8 ± 4 mg/ml (mean ± SD, $n = 4$). EC_{50} value for Ti-MPs could not be determined at the concentration <999 mg/ml and no higher concentrations of Ti-MPs were used.

3.2.2. Cell death

Compared to the medium (including 6% dead cells), Ti-NPs caused 9% and 19% increase in cell death at the concentration of 284 μg/ml (1/10 EC_{50}, $p < 0.01$) and 1420 μg/ml (1/2 EC_{50}, $p < 0.001$), respectively. There is no significant difference for Ti-NPs at the lower concentrations 1/50 and 1/100 EC_{50} compared to medium.

NiTi-MPs induced 9% more cell death ($p < 0.01$) at the concentration of 20,900 μg/ml (1/2 EC_{50}) compared to medium. No significant difference was found at 1/10 EC_{50}, 1/50 EC_{50} and 1/100 EC_{50}.

Ti-MPs only caused 9% increase ($p < 0.05$) of dead cells at the highest concentration (33,300 μg/ml) compared to medium. No significant difference was found at lower concentrations.

3.3. DNA damage

Comet assay results for Ti-NPs, Ti-MPs and NiTi-MPs in PDL-hTERT cells are shown in Fig. 1.

A significant increase in OTM value (compared to negative control) was detected after Ti-NPs exposure at all concentrations ($p < 0.01$). The mean OTM value for Ti-NPs at 1/10 EC_{50} (284 μg/ml) was significantly higher compared to 1/50 EC_{50},

Table 2 – Particle size distributions of Ti-NPs, NiTi-MPs and Ti-MPs (mean ± SD).

Particles	Particle size distribution (%)			
Ti-NPs	20–50 nm	50–100 nm	100–200 nm	>200 nm
	16.5 ± 4.9	73.1 ± 4.2	9.8 ± 1.7	0.6 ± 0.25
NiTi-MPs	<1 μm	1–5 μm	5–10 μm	>10 μm
	4.38 ± 0.75	12.50 ± 2.7	22.50 ± 3.0	60.60 ± 3.6
Ti-MPs	<1 μm	1–5 μm	5–10 μm	>10 μm
	11.63 ± 0.63	42.25 ± 2.99	24.5 ± 0.91	20.38 ± 2.02

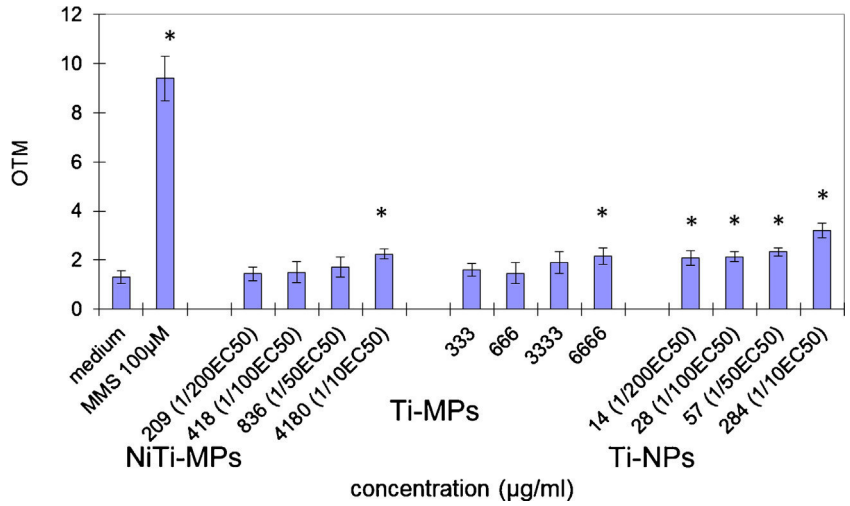

Fig. 1 – Comet assay result for Ti-NPs, NiTi-MPs and Ti-MPs. *Significantly different ($p < 0.05$) to negative control (medium).

1/100 EC_{50} and 1/200 EC_{50} ($p < 0.01$). No significant difference was detected among 1/50 EC_{50}, 1/100 EC_{50} and 1/200 EC_{50}. A significant increase in OTM value ($p < 0.001$) was observed at the concentration of 4180 μg/ml (1/10 EC_{50}) after NiTi-MPs exposure compared to negative control. Ti-MPs induced a significant increase in OTM value ($p < 0.001$) at the concentration of 6666 μg/ml, but no significant difference at the lower concentrations (3333 μg/ml, 666 μg/ml and 333 μg/ml).

In addition, the OTM value of Ti-NPs at the concentration of 284 μg/ml (1/10 EC_{50}) was 1.5 times higher than OTM value of NiTi-MPs at the concentration of 4180 μg/ml (1/10 EC_{50}). 284 μg/ml (1/10 EC_{50}) of Ti-NPs induced a significantly higher OTM value compared to Ti-MPs at 6666 μg/ml ($p < 0.001$).

3.4. *Cellular uptake*

3.4.1. *LSCM measurement*

Ti-NPs could be detected in the cytoplasm and nucleus of PDL-hTERT cells (Fig. 2). For NiTi-MPs and Ti-MPs, particles around 1 μm were found in the PDL-hTERT cells. No particles were detected in the nucleus (Figs. 3 and 4).

Table 3 – EC_{50} values (mean ± SD) and relative toxicity of Ti-NPs, NiTi-MPs and Ti-MPs determined with XTT viability assay.

	EC_{50} (mg/ml)	Relative toxicity
Ti-NPs	2.84 ± 0.37	352
NiTi-NPs	41.8 ± 4	24
Ti-MPs	>999	1

The cellular uptake efficiency of Ti-NPs, Ti-MPs and NiTi-MPs was determined by LSCM with different concentrations, as shown in Table 4. The ratio of cells with Ti-NPs inside the cytoplasm significantly increased ($p < 0.05$) when the exposure concentration of Ti-NPs was raised from 28 μg/ml (1/100 EC_{50}) to 56 μg/ml (1/50 EC_{50}). The ratio of cells with Ti-NPs in the nucleus also increased significantly from 5.0 ± 1.5% (mean ± SD, $n = 4$) to 11% ± 1.3% (mean ± SD, $n = 4$) when the concentration was increased. For NiTi-MPs, no significant difference was found in the cellular uptake efficiency when the exposure concentration was increased from 418 to 4180 μg/ml. For Ti-MPs (418 μg/ml), 33% ± 4.5% (mean ± SD, $n = 4$) of detected cells were found with Ti-MPs in the cytoplasm.

Table 4 – Cellular uptake efficiency of Ti-NPs, NiTi-MPs and Ti-MPs.

	Ratio of cells with particles in cytoplasm	Ratio of cells with particles in nucleus
Ti-NPs		
28 μg/ml (1/100 EC_{50})	58% ± 3.6	5.0% ± 1.5
56 μg/ml (1/50 EC_{50})	66% ± 3.0	11% ± 1.3
NiTi-MPs		
418 μg/ml (1/100 EC_{50})	11% ± 2.0	0%
4180 μg/ml (1/10 EC_{50})	10% ± 0.8	0%
Ti-MPs		
418 μg/ml	33% ± 4.5	0%

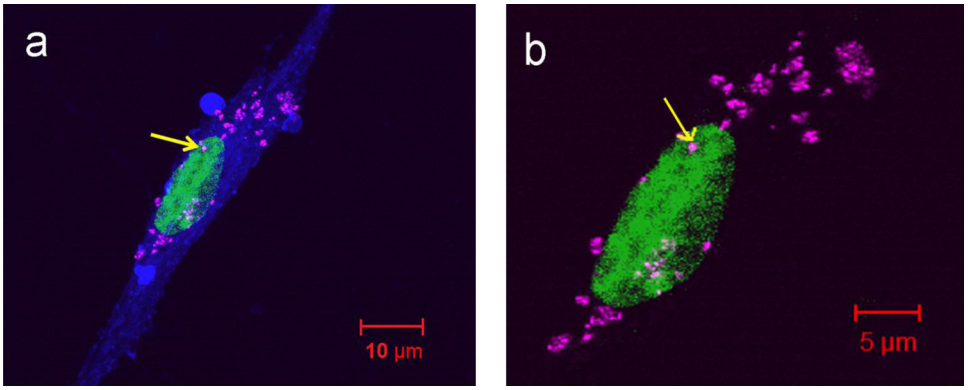

Fig. 2 – (a) LSCM image of a PDL-hTERT cell after exposure to Ti-NPs (28 µg/ml) for 24 h (z-stack slices merged into one image). Ti-NPs: pink, cell plasma membrane: blue, nucleus: green, yellow arrow: Ti-NP in the nucleus. (b) LSCM image of the nucleus of the same cell in (a). Ti-NPs: pink, nucleus: green, yellow arrow: Ti-NP in the nucleus. (For interpretation of the references to color in this figure legend, the reader is referred to the web version of this article.)

3.4.2. *TEM measurement*

The cellular uptake of Ti-NPs in PDL-hTERT cells was confirmed with TEM (Fig. 5). After exposure to 28 µg/ml (1/10 EC_{50}) of Ti-NPs for 24 h, particles between 30 nm and 200 nm were detected inside the cytoplasm.

Particle morphology of Ti-NPs in Fig. 6 shows that Ti-NPs can agglomerate, so particles/agglomerates with a size of 20–250 nm were observed.

4. Discussion

In this study, the toxic potential of Ti-NPs, Ti-MPs and NiTi-MPs in PDL-hTERT cells was measured and compared according to their particle size and cellular uptake efficiency.

4.1. *Particle size measurement*

According to the manufacturer, Ti-MPs and TiNi-MPs have a particle size below 325 mesh, this corresponds to a particle size of below 44 µm, and Ti-NPs have a particle size below 100 nm. Analysis of Ti-MPs with SEM verified stated data of manufacturer, while analysis of NiTi-MPs showed around 1% of particles with a size above 44 µm. There is no explanation in literature for the existence of these larger particles. Analysis of Ti-NPs also disagreed with manufacturer's data. SEM-measurement showed that besides Ti-NPs below 100 nm, Ti particles/agglomerates sized above 100 nm were found. For measurement of intracellular uptake of Ti-NPs, dimensions of particles were checked again with TEM: Results also showed agglomeration of particles resulting in sizes above 100 nm. In previous studies it was described that agglomeration is a common property of nanoparticles, which is due to the cohesive forces between primary nanoparticles [48]. For other materials (e.g. CuO, AgO, TiO_2, Cu, Al, Al_2O_3) studies showed that metal and metal oxide nanoparticles tend to form large agglomerates above 100 nm in liquid medias [31,49].

Clinical studies indicated that particles of Ti and Ti alloys ranging from 0.01 µm to 50 µm can be released into human body from Ti-based implants or replacements [25,26] and animal studies demonstrated the presence of Ti particles/debris sized between 3 µm and 250 µm in the peri-implant bone or tissues [23,24]. The particle sizes of our investigated particles are in that range.

4.2. *Cytotoxicity: XTT assay and cell death*

It was reported that Fe_2O_3-, Fe_3O_4- and TiO_2-NPs showed no significantly different cytotoxicity compared to their corresponding MPs in A549 cells at the same concentration (40 µg/cm^2) [31]. However, it was found that CuO- and ZnO-NPs induced higher cytotoxicity than their corresponding MPs [31,32]: CuO-NPs showed a 2-fold increase of cytotoxicity in A549 cells compared to CuO-MPs at the same concentration (40 µg/cm^2) (trypan blue exclusion test) [31]; after exposure to

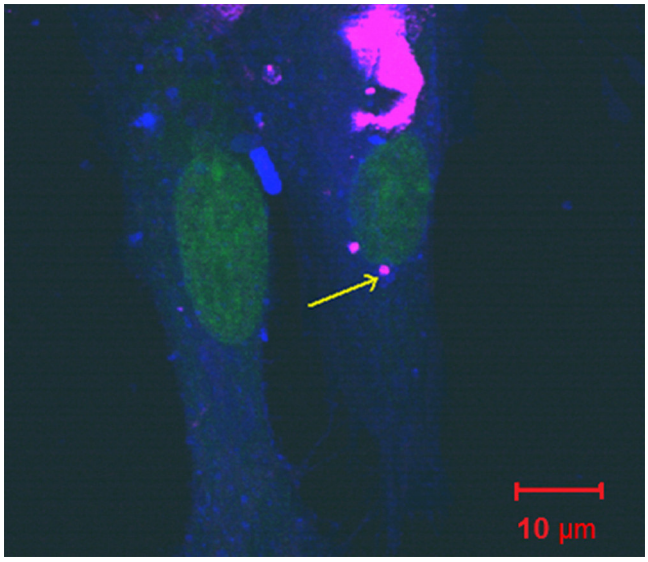

Fig. 3 – LSCM image of a PDL-hTERT cell after exposure to NiTi-MPs (418 µg/ml) for 24 h (z-stack slices merged into one image). NiTi-MPs: pink, cell plasma membrane: blue, nucleus: green, yellow arrow: NiTi-MP in the cell. (For interpretation of the references to color in this figure legend, the reader is referred to the web version of this article.)

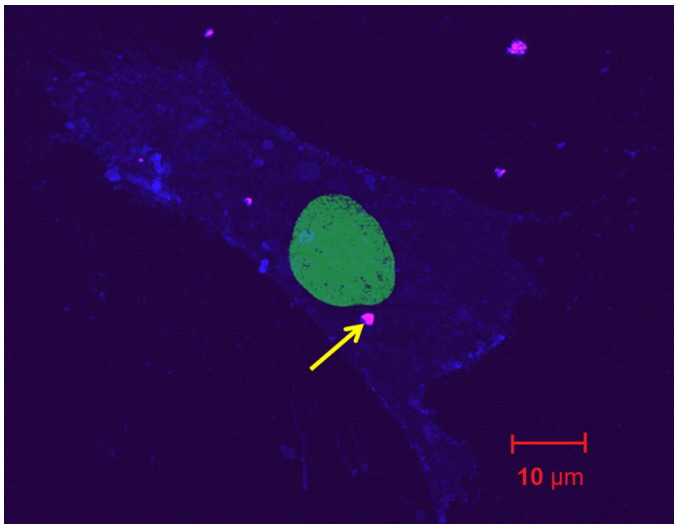

Fig. 4 – LSCM image of a PDL-hTERT cell after exposure to Ti-MPs (418 µg/ml) for 24 h (z-stack slices merged into one image). Ti-MPs: pink, cell plasma membrane: blue, nucleus: green, yellow arrow: Ti-MP in the cell. (For interpretation of the references to color in this figure legend, the reader is referred to the web version of this article.)

50 µg/ml of ZnO-NPs within 24 h, MTT (3-[4,5-dimethylthiazol-2-yl]-2,5 diphenyl tetrazolium bromide) assay and trypan blue exclusion test results indicated that around 50% of human nasal mucosa cells lost viability, whereas no loss of viability was detected for ZnO-MPs at the same concentration [32]. Furthermore it has been discussed that cytotoxicity of NPs can be induced by their large surface area per mass, release of toxic ions and ability to pass the cell membrane [32,50]. The results for cytotoxicity of Fe_2O_3-, Fe_3O_4- and TiO_2-particles might be explained by the fact that MPs used in the study above were mainly ≤1 µm and so could be taken up by cells just as their corresponding NPs. But particle sizes of CuO-MPs, ZnO-MPs (>1 µm) used in the study cited above are comparable to Ti-MPs investigated in present study.

XTT test and trypan blue exclusion test were used to measure the cytotoxicity of Ti-NPs, Ti-MPs and NiTi-MPs in PDL-hTERT cells. The results of XTT test indicated that the EC_{50} value of Ti-NPs (2.84 mg/ml) was more than 350-fold lower than the EC_{50} of Ti-MPs (>999 mg/ml). Therefore, Ti-NPs induced higher cytotoxicity than Ti-MPs, which is also confirmed by the trypan blue exclusion test: a significant increase in nonviable cells was observed after exposure to 0.28 mg/ml of Ti-NPs; 120-fold of this concentration (33.3 mg/ml) was required for Ti-MPs to get the same effect as after Ti-NPs exposure. So the present study for Ti-NPs and Ti-MPs is in accordance with the findings cited above, in which CuO- and ZnO-NPs caused higher cytotoxicity than their corresponding MPs [31,32].

4.3. *DNA damage*

In the present study, comet assay results indicated that 14 µg/ml of Ti-NPs induced a 1.5-fold increase in OTM value compared to negative control in PDL-hTERT cells; while a 500-fold concentration (6666 µg/ml) was required for Ti-MPs to get the same extent of DNA damage as after Ti-NPs exposure. The increase in OTM value is considered to be an indicator of DNA damage [42,43]; therefore, Ti-NPs displayed a 500-fold higher

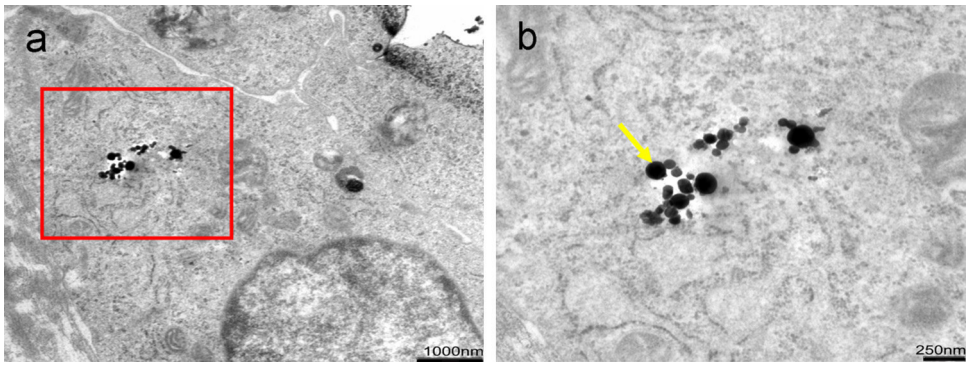

Fig. 5 – (a) TEM image of a PDL-hTERT cell after exposure to Ti-NPs (28 µg/ml) for 24 h. (b) Magnification of the marked area in (a). Yellow arrow: Ti-NPs (black) in the cell. (For interpretation of the references to color in this figure legend, the reader is referred to the web version of this article.)

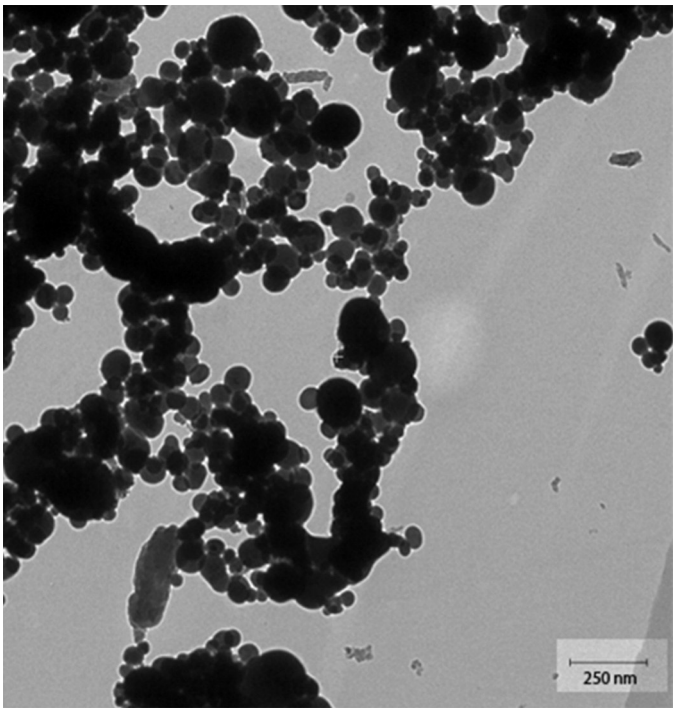

Fig. 6 – TEM image of Ti-NPs (agglomeration).

DNA damage potential compared to Ti-MPs. On the contrary, in previous studies Fe_2O_3 and TiO_2-NPs caused significantly ($p < 0.05$) less DNA damage (5% less in tail) compared to the corresponding MPs at the same concentrations [31]. But it was also described that NPs such as ZnO or CuO, induced more DNA damage than their corresponding MPs: ZnO-NPs induced a significant increase in DNA damage in human nasal mucosa cells starting from the concentration of 10 μg/ml ($p < 0.05$), in comparison to the negative control, while no DNA damage was observed with ZnO-MPs at the same concentration [32]; a 4-h exposure to CuO-NPs (40 μg/cm^2) induced 4 times more DNA damage in A549 cells compared to the control group, same concentration of CuO-MPs only caused 0.5-fold more DNA damage [31]. So in the present study the results for Ti particles agree with the results cited above for ZnO and CuO.

4.4. *Cellular uptake*

In the present study, LSCM results showed that after exposure to Ti-NPs (28 μg/ml), about 60% of investigated cells were found containing Ti-NPs. Therefore, Ti-NPs had the highest cellular uptake efficiency, compared to Ti-MPs and TiNi-MPs. The higher cellular uptake efficiency of Ti-NPs compared to Ti-MPs indicates that the uptake of Ti particles in PDL-hTERT cells is also size-dependent. This result for Ti-NPs is in line with previous studies. These former studies reported that non-phagocytic eukaryotic cells could take up particles that are below 1 μm [51], and the cellular uptake efficiency of nanoparticles can be affected by particle size [35,36,52]: the intracellular uptake efficiency of silica nanoparticles for Hela cells is size dependent in the order of 55.64 nm > 167.84 nm > 307.6 nm [35]. The intracellular uptake efficiency of gold NPs in human breast cancer SK-BR-3 cells was also influenced by the particle size, a maximal uptake was mediated by particles of 40–50 nm [36]. It was found that poly (lactic-co-glycolic acid) (PLGA) particles in size of 100 nm induced 1.7 and 5.8 times higher uptake efficiency compared to 1 μm- and 10 μm-PLGA particles in Caco-2 cells, respectively [52].

In the present study, in addition to the detected highest cellular uptake efficiency, the highest cytotoxicity was also determined for Ti-NPs compared to Ti-MPs and NiTi-MPs. Similar result has been reported by a previous study, where toxicity of Silica-Titania Hollow NPs (SiTi-NPs) in macrophages has been correlated to the cellular uptake efficiency: cationic SiTi-NPs (50 nm) induced the highest uptake efficiency and also the most toxic effects (e.g. cytotoxicity) on macrophages J774A.1 cells compared to other SiTi-NPs with different sizes and coating surfaces [35]. Furthermore, results of present study showed that only Ti-NPs were found in the nucleus and Ti-NPs induced more DNA damage compared to Ti-MPs and NiTi-MPs. So the higher potential of DNA damage for NPs might also be explained by the nuclear uptake of NPs.

Particles can be taken up by cells via endocytosis which includes phagocytosis and pinocytosis [53]. Through phagocytosis, large particles with diameters exceeding 750 nm can be taken up, but it occurs only in specific cells such as macrophages, neutrophils and monocytes [53]. Pinocytosis occurs in all cell types and four mechanisms of pinocytosis were reported: macropinocytosis (vesicle size >1 μm), clathrin-mediated endocytosis (vesicle size is around 120 nm), caveolae-mediated endocytosis (vesicle size is 60 nm) and clathrin- and caveolae-independent endocytosis (vesicle size is 90 nm) [53,54]. A previous study showed that silica particles (307.6 nm) were taken up by Hela cells mainly via clathrin-mediated endocytosis [35], although this particle size

(307.6 nm) is 2.5 times larger than the vesicle size (120 nm) of clathrin-mediated endocytosis. It was found that smaller silica particles (56 nm) can also be taken up by caveolae mediated endocytosis (60 nm) except by clathrin-mediated endocytosis (120 nm) [35]. In the present study, for Ti-MPs no EC_{50} could be determined at the concentration of 999 mg/ml, so cellular uptake efficiency of Ti-MPs at different concentrations was not compared. The cellular uptake efficiency of the Ti-NPs increased by 8% when the exposure concentration was improved from 28 μg/ml to 56 μg/ml, but the cellular uptake efficiency of NiTi-MPs did not significantly increase even when the exposure concentration was increased from 418 μg/ml to 4180 μg/ml. Obviously, Ti-NPs and NiTi-MPs can be taken up through different uptake mechanisms: with the size of 20–250 nm, Ti-NPs could be taken up by both caveolae mediated endocytosis (60 nm) and clathrin-mediated endocytosis (120 nm); NiTi-MPs (0.7–90 μm) might be taken up by the clathrin-mediated endocytosis (120 nm).

In the present study, after PDL-hTERT cells were exposed to Ti-NPs (20–250 nm), about 4 to 15-times larger Ti particles with a size between 0.3 and 1 μm were found in the nucleus. Similarly, Cronholm et al. reported that after exposure to Ag-NPs (20–200 nm), particles between 0.5 and 1 μm were detected in the nucleus of A549 cells [44]. It was reported that the nuclear bidirectional transport of macromolecules between the nucleus and the cytoplasm could occur through the nuclear pore complexes (NPCs) with a diameter of 40–50 nm [55,56]. It was found that macromolecules such as cargo-receptor-gold complexes with a diameter up to 40 nm were able to be transported through NPCs [55]. Considering the literature cited above [55,56], in the present study Ti particles (0.3–1 μm) found in the nucleus are too large to be transported through NPCs. Additionally, it was found that Ti-NPs can form agglomerates larger than 100 nm (Fig. 6). Two explanations for finding such large Ti particles in the nucleus might be given: (1) the larger particles (0.3–1 μm) in the nucleus might be agglomerates formed by each Ti-NP (20–50 nm) that is able to go through nuclear pores; (2) the agglomeration of Ti-NPs occurs in the cytoplasm and then the agglomerates are transported into the nucleus via vesicles lodged to the nucleus. The second explanation is in accordance with previous study on Ag-NPs suggesting also that Ag-NPs can be transported with vesicles [54].

In the present study, NiTi-MPs (EC_{50} = 42 mg/ml) mediated more than 24-times cytotoxicity compared to Ti-MPs (EC_{50} > 999 mg/ml). Considering the size distribution of NiTi-MPs and Ti-MPs (Table 2), 17% of NiTi-MPs were below 5 μm, while 54% of Ti-MPs were below 5 μm, and meanwhile, Ti-MPs induced 2-fold higher cellular uptake efficiency, this higher cytotoxicity (24-fold) of NiTi could be explained by the toxic potential of Ni. In previous studies, the adverse effects of Ni have been reported: Ni is not only known as an allergen but also a possible immunotoxic agent in humans [57,58] and it was found that Ni (2.5 ng/ml) released from Ni-containing fixed orthodontic appliances could cause cytotoxicity and DNA damage in oral mucosa cells [22]. Therefore, the toxic effects of investigated particles (Ti-NPs, Ti-MPs and NiTi-MPs) might depend not only on the particle size and cellular uptake efficiency, but also on the chemical composition such as the alloy NiTi.

5. Conclusion

Compared to Ti-MPs and NiTi-MPs, Ti-NPs induced higher cellular uptake efficiency and higher toxic potential in PDL-hTERT cells. Ni in the alloy NiTi induced an increase in the toxic potential compared to Ti-MPs.

Acknowledgements

This study was financially supported by China Scholarship Council (CSC). We would like to thank Ms Renate Scheler, Ms Sabine Schäfer and Ms Martina Hitzenbichler for TEM measurement and Mr Stefan Schulz for the technical assistance.

REFERENCES

[1] Okabe T, Hero H. The use of titanium in dentistry. Cells Mater (U S A) 1995;5:211–30.
[2] Watanabe K, Miyakawa O, Takada Y, Okuno O, Okabe T. Casting behavior of titanium alloys in a centrifugal casting machine. Biomaterials 2003;24:1737–43.
[3] Lautenschlager EP, Monaghan P. Titanium and titanium alloys as dental materials. Int Dent J 1993;43:245–53.
[4] Özcan M, Hämmerle C. Titanium as a reconstruction and implant material in dentistry: advantages and pitfalls. Materials 2012;5:1528–45.
[5] Castilho GA, Martins MD, Macedo WA. Surface characterization of titanium based dental implants. Braz J Phys 2006;36:1004–8.
[6] Elias C, Lima J, Valiev R, Meyers M. Biomedical applications of titanium and its alloys. JOM 2008;60:46–9.
[7] Thompson SA. An overview of nickel–titanium alloys used in dentistry. Int Endod J 2000;33:297–310.
[8] Setcos JC, Babaei-Mahani A, Silvio LD, Mjor IA, Wilson NH. The safety of nickel containing dental alloys. Dent Mater 2006;22:1163–8.
[9] Valiev RZ, Semenova IP, Latysh VV, Rack H, Lowe TC, Petruzelka J, et al. Nanostructured titanium for biomedical applications. Adv Eng Mater 2008;10:B7–15.
[10] Lalor PA, Revell PA, Gray AB, Wright S, Railton GT, Freeman MA. Sensitivity to titanium. A cause of implant failure? J Bone Joint Surg Br 1991;73:25–8.
[11] Sicilia A, Cuesta S, Coma G, Arregui I, Guisasola C, Ruiz E, et al. Titanium allergy in dental implant patients: a clinical study on 1500 consecutive patients. Clin Oral Implants Res 2008;19:823–35.
[12] Egusa H, Ko N, Shimazu T, Yatani H. Suspected association of an allergic reaction with titanium dental implants: a clinical report. J Prosthet Dent 2008;100:344–7.
[13] Voggenreiter G, Leiting S, Brauer H, Leiting P, Majetschak M, Bardenheuer M, et al. Immuno-inflammatory tissue reaction to stainless-steel and titanium plates used for internal fixation of long bones. Biomaterials 2003;24:247–54.
[14] Hansen DC. Metal corrosion in the human body: the ultimate bio-corrosion scenario. Electrochem Soc Interface 2008;17:31.
[15] Yang J, Merritt K. Detection of antibodies against corrosion products in patients after Co–Cr total joint replacements. J Biomed Mater Res 1994;28:1249–58.
[16] Okazaki Y, Gotoh E. Comparison of metal release from various metallic biomaterials in vitro. Biomaterials 2005;26:11–21.

[17] Jacobs JJ, Silverton C, Hallab NJ, Skipor AK, Patterson L, Black J, et al. Metal release and excretion from cementless titanium alloy total knee replacements. Clin Orthop Relat Res 1999:173–80.
[18] Browne M, Gregson PJ. Effect of mechanical surface pretreatment on metal ion release. Biomaterials 2000;21:385–92.
[19] Bianco PD, Ducheyne P, Cuckler JM. Systemic titanium levels in rabbits with a titanium implant in the absence of wear. J Mater Sci Mater Med 1997;8:525–9.
[20] Woodman JL, Jacobs JJ, Galante JO, Urban RM. Metal ion release from titanium-based prosthetic segmental replacements of long bones in baboons: a long-term study. J Orthop Res 1984;1:421–30.
[21] Soto-Alvaredo J, Blanco E, Bettmer J, Hevia D, Sainz RM, Lopez Chaves C, et al. Evaluation of the biological effect of Ti generated debris from metal implants: ions and nanoparticles. Metallomics 2014;6:1702–8.
[22] Faccioni F, Franceschetti P, Cerpelloni M, Fracasso ME. In vivo study on metal release from fixed orthodontic appliances and DNA damage in oral mucosa cells. Am J Orthod Dentofacial Orthop 2003;124:687–93 [discussion 93-4].
[23] Martini D, Fini M, Franchi M, Pasquale VD, Bacchelli B, Gamberini M, et al. Detachment of titanium and fluorohydroxyapatite particles in unloaded endosseous implants. Biomaterials 2003;24:1309–16.
[24] Franchi M, Bacchelli B, Martini D, Pasquale VD, Orsini E, Ottani V, et al. Early detachment of titanium particles from various different surfaces of endosseous dental implants. Biomaterials 2004;25:2239–46.
[25] Urban RM, Jacobs JJ, Tomlinson MJ, Gavrilovic J, Black J, Peoc'h M. Dissemination of wear particles to the liver, spleen, and abdominal lymph nodes of patients with hip or knee replacement. J Bone Joint Surg Am 2000;82:457–76.
[26] Urban RM, Jacobs JJ, Sumner DR, Peters CL, Voss FR, Galante JO. The bone-implant interface of femoral stems with non-circumferential porous coating. J Bone Joint Surg Am 1996;78:1068–81.
[27] Pioletti DP, Takei H, Kwon SY, Wood D, Sung KL. The cytotoxic effect of titanium particles phagocytosed by osteoblasts. J Biomed Mater Res 1999;46:399–407.
[28] Lohmann CH, Schwartz Z, Koster G, Jahn U, Buchhorn GH, MacDougall MJ, et al. Phagocytosis of wear debris by osteoblasts affects differentiation and local factor production in a manner dependent on particle composition. Biomaterials 2000;21:551–61.
[29] Wang ML, Nesti LJ, Tuli R, Lazatin J, Danielson KG, Sharkey PF, et al. Titanium particles suppress expression of osteoblastic phenotype in human mesenchymal stem cells. J Orthop Res 2002;20:1175–84.
[30] Wang ML, Tuli R, Manner PA, Sharkey PF, Hall DJ, Tuan RS. Direct and indirect induction of apoptosis in human mesenchymal stem cells in response to titanium particles. J Orthop Res 2003;21:697–707.
[31] Karlsson HL, Gustafsson J, Cronholm P, Moller L. Size-dependent toxicity of metal oxide particles – a comparison between nano- and micrometer size. Toxicol Lett 2009;188:112–8.
[32] Hackenberg S, Scherzed A, Technau A, Kessler M, Froelich K, Ginzkey C, et al. Cytotoxic, genotoxic and pro-inflammatory effects of zinc oxide nanoparticles in human nasal mucosa cells in vitro. Toxicol In Vitro 2011;25:657–63.
[33] Oh WK, Kim S, Choi M, Kim C, Jeong YS, Cho BR, et al. Cellular uptake, cytotoxicity, and innate immune response of silica-titania hollow nanoparticles based on size and surface functionality. ACS Nano 2010;4:5301–13.
[34] Lee KD, Nir S, Papahadjopoulos D. Quantitative analysis of liposome-cell interactions in vitro: rate constants of binding and endocytosis with suspension and adherent J774 cells and human monocytes. Biochemistry 1993;32:889–99.
[35] Zhu J, Liao L, Zhu L, Zhang P, Guo K, Kong J, et al. Size-dependent cellular uptake efficiency, mechanism, and cytotoxicity of silica nanoparticles toward HeLa cells. Talanta 2013;107:408–15.
[36] Jiang W, Kim BY, Rutka JT, Chan WC. Nanoparticle-mediated cellular response is size-dependent. Nat Nanotechnol 2008;3:145–50.
[37] Gault P, Black A, Romette JL, Fuente F, Schroeder K, Thillou F, et al. Tissue-engineered ligament: implant constructs for tooth replacement. J Clin Periodontol 2010;37:750–8.
[38] Choi BH. Periodontal ligament formation around titanium implants using cultured periodontal ligament cells: a pilot study. Int J Oral Maxillofac Implants 2000;15:193–6.
[39] Lin Y, Gallucci GO, Buser D, Bosshardt D, Belser UC, Yelick PC. Bioengineered periodontal tissue formed on titanium dental implants. J Dent Res 2011;90:251–6.
[40] Docheva D, Padula D, Popov C, Weishaupt P, Pragert M, Miosge N, et al. Establishment of immortalized periodontal ligament progenitor cell line and its behavioural analysis on smooth and rough titanium surface. Eur Cell Mater 2010;19:228–41.
[41] Van Landuyt KL, Yoshihara K, Geebelen B, Peumans M, Godderis L, Hoet P, et al. Should we be concerned about composite (nano-)dust? Dent Mater 2012;28:1162–70.
[42] Kleinsasser NH, Schmid K, Sassen AW, Harreus UA, Staudenmaier R, Folwaczny M, et al. Cytotoxic and genotoxic effects of resin monomers in human salivary gland tissue and lymphocytes as assessed by the single cell microgel electrophoresis (comet) assay. Biomaterials 2006;27:1762–70.
[43] Kleinsasser NH, Wallner BC, Harreus UA, Kleinjung T, Folwaczny M, Hickel R, et al. Genotoxicity and cytotoxicity of dental materials in human lymphocytes as assessed by the single cell microgel electrophoresis (comet) assay. J Dent 2004;32:229–34.
[44] Cronholm P, Karlsson HL, Hedberg J, Lowe TA, Winnberg L, Elihn K, et al. Intracellular uptake and toxicity of Ag and CuO nanoparticles: a comparison between nanoparticles and their corresponding metal ions. Small 2013;9:970–82.
[45] Tsai S-W, Chen Y-Y, Liaw J-W. Compound cellular imaging of laser scanning confocal microscopy by using gold nanoparticles and dyes. Sensors 2008;8:2306–16.
[46] Jain PK, Huang X, El-Sayed IH, El-Sayed MA. Noble metals on the nanoscale: optical and photothermal properties and some applications in imaging, sensing, biology, and medicine. Acc Chem Res 2008;41:1578–86.
[47] Doorn J, Fernandes HA, Le BQ, van de Peppel J, van Leeuwen JP, De Vries MR, et al. A small molecule approach to engineering vascularized tissue. Biomaterials 2013;34:3053–63.
[48] Yao W, Guangsheng G, Fei W, Jun W. Fluidization and agglomerate structure of SiO_2 nanoparticles. Powder Technol 2002;124:152–9.
[49] Murdock RC, Braydich-Stolle L, Schrand AM, Schlager JJ, Hussain SM. Characterization of nanomaterial dispersion in solution prior to in vitro exposure using dynamic light scattering technique. Toxicol Sci 2008;101:239–53.
[50] Midander K, Cronholm P, Karlsson HL, Elihn K, Moller L, Leygraf C, et al. Surface characteristics, copper release, and toxicity of nano- and micrometer-sized copper and copper(II) oxide particles: a cross-disciplinary study. Small 2009;5:389–99.
[51] Rejman J, Oberle V, Zuhorn IS, Hoekstra D. Size-dependent internalization of particles via the pathways of clathrin- and caveolae-mediated endocytosis. Biochem J 2004;377:159–69.
[52] Desai MP, Labhasetwar V, Walter E, Levy RJ, Amidon GL. The mechanism of uptake of biodegradable microparticles in

Caco-2 cells is size dependent. Pharm Res 1997;14:1568–73.
[53] Conner SD, Schmid SL. Regulated portals of entry into the cell. Nature 2003;422:37–44.
[54] AshaRani PV, Low Kah Mun G, Hande MP, Valiyaveettil S. Cytotoxicity and genotoxicity of silver nanoparticles in human cells. ACS Nano 2009;3:279–90.
[55] Pante N, Kann M. Nuclear pore complex is able to transport macromolecules with diameters of about 39 nm. Mol Biol Cell 2002;13:425–34.
[56] Frenkiel-Krispin D, Maco B, Aebi U, Medalia O. Structural analysis of a metazoan nuclear pore complex reveals a fused concentric ring architecture. J Mol Biol 2010;395:578–86.
[57] Das KK, Das SN, Dhundasi SA. Nickel its adverse health effects & oxidative stress. Indian J Med Res 2008;128:412–25.
[58] Bando K, Kinbara TH, Tanaka M, Kuroishi Y, Sasaki T, Takano-Yamamoto K, et al. Resin monomers act as adjuvants in Ni-induced allergic dermatitis in vivo. J Dent Res 2014;93:1101–7.

7.2 Further publications

Schuster L, Rothmund L, **He X**, Van Landuyt KL, Schweikl H, Hellwig E, Carell T, Hickel R, Reichl FX, Högg C. Effect of Opalescence(R) bleaching gels on the elution of dental composite components. Dent Mater. 2015; 31:745-57.

Schuster L, Reichl FX, Rothmund L, **He X**, Yang Y, Van Landuyt KL, Kehe K, Polydorou O, Hickel R, Högg C. Effect of Opalescence (R) bleaching gels on the elution of bulk-fill composite components. Dent Mater. 2016; 32:127-35.

Högg C, Maier M, Dettinger-Maier K, **He X**, Rothmund L, Kehe K, Hickel R, Reichl FX. Effect of various light curing times on the elution of composite components. Clinical oral investigations. 2015; 1-9.

8 Acknowledgement

This dissertation was completed at the Department of Operative/Restorative Dentistry, Periodontology and Pedodontics, LMU and Walther-Straub-Institute of Pharmacology and Toxicology, LMU and it was supported by a joint scholarship project of the Ludwig Maximilian University of Munich and the China Scholarship Council.

Many people have supported and helped in valuable ways to conduct this work, to which I really want to give my sincere appreciation. First and foremost, I will express my sincerest gratitude to my advisor Prof. Dr. Franz-Xaver Reichl for his continuous support and guidiance of my study, and also for his patience and kindness. In the last 4 years, his support and encouragement has helped me to overcome all the difficulties in my study, i feel so fortunate to have Prof Reichl as my advisor.

Furthermore, I would like to thank Professor Bernhard Michalke and Professor Stefan Milz for their technique support in analytic measurements, histological analysis and sample-cutting preparation, and I am also very grateful for the valuable suggestions and kind help they offered me.

At the same time, I want to thank Dr Christof Hoegg, who has been always there to listen to me and give me constructive advices for my experiments and paper writing when i am in need. Also many thanks to my colleages Mr Stefan Schulz, Mr Yang Yang and Ms Yan Wang, i really appreciate all the help and support they offered me in both life and study.

Besides, I want to express my appreciation to all the other people who once offered help to me, such as Ms Renate Scheler in Eye clinic in LMU Munich, Ms Bärbel Benker and Mr Peter Grill in Helmholtz Zentrum Munich.

At last, I would like to give my sincere thanks to my famillies, especially to my parents and my husband Xiao Wu, it is their continuous support and love making me move forward and fullfill my dreams.

9 Curriculum Vitae

Xiuli He

Personal information:

Date and place of birth:	20.02.1986 in Shandong, China
Nationality:	China

Education:

09.2012 – now	Doctoral study in Department of Operative/Restorative Periodontology and Pedodontics, and Walther Straub Institute of Pharmacology and Toxicology, LMU
09.2009 – 06.2012	Master study about Biology in State Key Laboratory of Microbial Technology in Shandong University, China
09.2005 – 06.2009	Bachelor study about Biology/Food quality and safety in the department of Life Science in Shandong Normal University, China

Publications:

He X, *Reichl FX, Wang Y, Michalke B, Milz S, Yang Y, Stolper P, Lindemaier G, Graw M, Hickel R, Högg C. Analysis of titanium and other metals in human jawbones with dental implants – A case series study. Dent Mater. 2016; 32:1042-51.*

He X, *Hartlieb E, Rothmund L, Waschke J, Wu X, Van Landuyt KL, Milz S, Michalke B, Hickel R, Reichl FX, Högg C. Intracellular uptake and toxicity of three different Titanium particles. Dent Mater. 2015; 31(6):734-44.*

Schuster L, Rothmund L, ***He X****, Van Landuyt KL, Schweikl H, Hellwig E, Carell T, Hickel R, Reichl FX, Högg C. Effect of Opalescence(R) bleaching gels on the elution of dental composite components. Dent Mater. 2015; 31:745-57.*

Högg C, Maier M, Dettinger-Maier K, ***He X****, Rothmund L, Kehe K, Hickel R, Reichl FX. Effect of various light curing times on the elution of composite components. Clinical oral investigations. 2015; 1-9.*

Schuster L, Reichl FX, Rothmund L, ***He X****, Yang Y, Van Landuyt KL, Kehe K, Polydorou O, Hickel R, Högg C. Effect of Opalescence (R) bleaching gels on the elution of bulk-fill composite components. Dent Mater. 2016; 32:127-35.*

Eidesstattliche Versicherung

He, Xiuli

Name, Vorname

Ich erkläre hiermit an Eides statt,

dass ich die vorliegende Dissertation mit dem Thema

Ti release from dental implants in human jawbone and the toxicity and cellular uptake of Ti particles in human cells

selbständig verfasst, mich außer der angegebenen keiner weiteren Hilfsmittel bedient und alle Erkenntnisse, die aus dem Schrifttum ganz oder annähernd übernommen sind, als solche kenntlich gemacht und nach ihrer Herkunft unter Bezeichnung der Fundstelle einzeln nachgewiesen habe.

Ich erkläre des Weiteren, dass die hier vorgelegte Dissertation nicht in gleicher oder in ähnlicher Form bei einer anderen Stelle zur Erlangung eines akademischen Grades eingereicht wurde.

Munich, 21.07.2016

Ort, Datum

Unterschrift Doktorandin/Doktorand